

## Use Authorization

In presenting this dissertation in partial fulfillment of the requirements for an advanced degree at Idaho State University, I agree that the Library shall make it freely available for inspection. I further state that permission for extensive copying of my dissertation for scholarly purposes may be granted by the Dean of the Graduate School, Dean of my academic division, or by the University Librarian. It is understood that any copying or publication of this dissertation for financial gain shall not be allowed without my written permission.

Signature \_\_\_\_\_

Date \_\_\_\_\_

PLUTONIUM-239 SYSTEMIC BIOKINETIC MODEL FOR RATS

by

Robert Thomas Etnire

A dissertation

submitted in partial fulfillment

of the requirements for the degree of

Doctor of Philosophy in the Department of Nuclear Science and Engineering

Idaho State University

August 2020

To the Graduate Faculty:

The members of the committee appointed to examine the dissertation of Robert Thomas Etnire find it satisfactory and recommend that it be accepted.

---

Dr. Richard R. Brey,  
Major Advisor

---

Dr. Thomas F. Gesell,  
Committee Member

---

Dr. Chad L. Pope,  
Committee Member

---

Dr. Scott C. Miller,  
Committee Member

---

Dr. DeWayne R. Derryberry,  
Graduate Faculty Representative

## TABLE OF CONTENTS

LIST OF FIGURES .....	vi
LIST OF TABLES .....	ix
LIST OF ABBREVIATIONS.....	x
ABSTRACT.....	xii
CHAPTER 1 INTRODUCTION .....	1
CHAPTER 2 LITERATURE REVIEW .....	4
Plutonium.....	4
Biokinetic Models.....	6
Animal Studies.....	17
Akaike's Information Criterion.....	21
CHAPTER 3 DATA .....	23
Animals and Animal Care.....	23
Experimental Study.....	24
Radioanalysis .....	24
Material Balance .....	25
CHAPTER 4 MATERIALS AND METHODS .....	26
Rat Model.....	26
Modeling Software.....	30
Statistical Method .....	32
Hypothesis.....	33
CHAPTER 5 RESULTS .....	35
First Compartmental Model.....	36
Reduced Compartmental Model .....	45
Two Liver Compartmental Model .....	52
$\Delta$ AIC .....	57
CHAPTER 6 DISCUSSION.....	59
CHAPTER 7 CONCLUSION.....	61

REFERENCES .....	62
APPENDIX A.....	66

## LIST OF FIGURES

Figure 1. Compartments and directions of movement of Pu (Leggett 1985) .....	8
Figure 2. ICRP 67 biokinetic model (ICRP 1993).....	10
Figure 3. Optimized version of the ICRP 67 model for plutonium with Polig's skeletal model and affected gastrointestinal compartments (Luciani and Polig 2000) .....	13
Figure 4. Structure of proposed model (Leggett et al. 2005).....	15
Figure 5. Compartment model of Pu transport and uptake in tissues of the rat 0.25-18 hr after IV injection of $^{239}\text{Pu(IV)}$ citrate (Durbin 1972) .....	19
Figure 6. The initial model that will be used to assess the fit of the data .....	27
Figure 7. Simplified version of the rat model .....	28
Figure 8. Complexities introduced to the rat model .....	29
Figure 9. Further compartments added to the rat model.....	30
Figure 10. First model constructed in SAAM II.....	36
Figure 11. Semilog plot of blood sample in first constructed model.....	39
Figure 12. Semilog plot of skeleton sample in first constructed model.....	39
Figure 13. Semilog plot of liver sample in first constructed model.....	40
Figure 14. Semilog plot of soft tissue sample in first constructed model.....	40
Figure 15. Semilog plot of kidneys sample in first constructed model .....	41
Figure 16. Semilog plot of urine sample in first constructed model.....	41

Figure 17. Semilog plot of gonads sample in first constructed model.....	42
Figure 18. Semilog plot of GI sample in first constructed model.....	42
Figure 19. Semilog plot of feces sample in first constructed model.....	43
Figure 20. Semilog plot of pelt sample in first constructed model.....	43
Figure 21. Semilog plot of spleen sample in first constructed model.....	44
Figure 22. Semilog plot of lung sample in first constructed model.....	44
Figure 23. Semilog plot of muscle sample in first constructed model.....	45
Figure 24. Reduced compartmental model .....	46
Figure 25. Semilog plot of blood sample in reduced compartment model .....	48
Figure 26. Semilog plot of liver sample in reduced compartment model.....	48
Figure 27. Semilog plot of kidneys sample in reduced compartment model.....	49
Figure 28. Semilog plot of GI sample in reduced compartment model.....	49
Figure 29. Semilog plot of soft tissue sample in reduced compartment model.....	50
Figure 30. Semilog plot of urine sample in reduced compartment model.....	50
Figure 31. Semilog plot of feces sample in reduced compartment model.....	51
Figure 32. Semilog plot of skeleton sample in reduced compartment model.....	51
Figure 33. Two liver compartment model .....	52
Figure 34. Semilog plot of blood sample in two liver compartment model .....	54

Figure 35. Semilog plot of liver sample in two liver compartment model .....	54
Figure 36. Semilog plot of kidneys sample in two liver compartment model .....	55
Figure 36. Semilog plot of GI sample in two liver compartment model .....	55
Figure 38. Semilog plot of soft tissue sample in two liver compartment model .....	56
Figure 39. Semilog plot of urine sample in two liver compartment model .....	56
Figure 40. Semilog plot of feces sample in two liver compartment model .....	57
Figure 41. Semilog plot of skeleton sample in two liver compartment model .....	57
Figure A.1. Two kidneys compartment model .....	67
Figure A.2. Two soft tissue compartment model.....	68
Figure A.3. Multiple complexities compartment model.....	70

## LIST OF TABLES

Table 1. Half-life, decay modes, and radioactive decay products of selected plutonium isotopes (Shleien et al. 1998) .....	5
Table 2. Decay chain and branching fractions of <sup>239</sup> Pu (ICRP 2008).....	6
Table 3. ICRP 67 transfer rates in adults for plutonium (ICRP 1993) .....	11
Table 4. Transfer rates of the optimized plutonium biokinetic model in adults (Luciani and Polig 2000) .....	14
Table 5. Baseline parameter values for a typical healthy adult (Leggett et al. 2005).....	16
Table 6. <sup>239</sup> Pu Material Balance Recoveries for the Experimental Groups in this Study .....	25
Table 7. Parameters for first model construction.....	38
Table 8. Parameters for reduced compartmental model .....	47
Table 9. Parameters for two liver compartmental model.....	53

## LIST OF ABBREVIATIONS

AIC	Akaike's Information Criteria
Bq	Becquerel
GI	gastrointestinal
hr	hours
ICRP	International Commission on Radiological Protection
IV	intravenously
JVC	jugular vein cannulated
LLI	lower large intestine
LRRI	Lovelace Respiratory Research Institute
LSC	liquid scintillation counter
MLE	maximum likelihood estimator
nCi	nanocurie
NCRP	National Council on Radiation Protection and Measurements
Pu	Plutonium
QC	quality control
SAAM II	Simulation, Analysis, and Modeling Software II

SD standard deviation

U Uranium

$\mu\text{L}$  microliter

ULI upper large intestine

## Plutonium-239 Systemic Biokinetic Model for Rats

Dissertation Abstract – Idaho State University (2020)

The goal of this research project is to build a  $^{239}\text{Pu}$  systemic biokinetic model for rats. While a rat model has been developed by Durbin (1972), it is not widely used. New animal data and research available on the biokinetics of plutonium and other radionuclides provided the necessary information that allowed the update to the ICRP 67 human model to be revised. The ICRP 67 model will act as the starting point for this research.

The data used for this project was collected from the experiment conducted at Lovelace Respiratory Research Institute. A total of 48 rats were injected with  $^{239}\text{Pu}$  citrate and placed into one of six groups which correlated to a predefined time period of when the rat would be sacrificed for data collection. Urine and feces were collected daily from each rat. Organ and tissue samples were collected after each group of rats were sacrificed at the time of their previously assigned group.

The modeling software used to build the rat model from the data collected during the experiment will be SAAM II. SAAM II is modeling and simulation software supporting statistical calibration of compartment models in various science disciplines with over 2,000 scientific publications. AIC is used as the statistical method to determine the quality of the compartment model. The ideal model is the one that minimizes the AIC value. The balance of determining the preferred model is one that introduces enough parameters for improving the goodness of fit without increasing complexities in order to produce a minimum AIC value. Multiple biokinetic models

were built in SAAM II and processed to determine their fit and AIC was used to assess the quality of the model in the goal of building a systemic biokinetic model for rats.

A reduced model does provide a better quality as defined by AIC, but there are still several compartments that do not have a good fit of the data. Not having as many complexities does seem to have better fits of each compartment. However, the reduced model does provide a starting point for future research in developing a  $^{239}\text{Pu}$  systemic biokinetic model for rats.

Keywords: plutonium; biokinetics; rat model; injection; liver; skeleton

## CHAPTER 1

### INTRODUCTION

Radiological protection is concerned with protecting individuals from the harmful effects of radiation and radioactive materials (ICRP 1990). This is done in a number of ways including understanding the multiple opportunities radioactive materials can enter the body which can occur either by ingestion, inhalation, injection, or through wounds. Depending on the route of entry into the body, the effects of the radionuclide can vary, as can the response needed in order to determine what intervention is necessary. Biokinetic models have been developed to help determine the transport of different radionuclides through the body, their deposition in specific organs and tissues, and their clearance from the body. The knowledge that these models are based on help in the radiological protection of the individual.

The International Commission on Radiological Protection (ICRP) and the National Council on Radiation Protection and Measurements (NCRP) have developed different biokinetic models over time. While ICRP has developed several biokinetic models over the years, they developed a new biokinetic model for humans presented in ICRP 67 scientific report which built upon the previous biokinetic model described in ICRP 56 in 1989. New research and data available on the biokinetics of plutonium and other radionuclides provided the necessary information that allowed the update to the ICRP 67 model to be revised (ICRP 1993). Although the original model presented in ICRP 56 and the revised model in ICRP 67 are for humans and the research used to develop these models are primarily based on animal data, there is not currently a widely used rat based

biokinetic model. Rats generally consist of the majority of plutonium based data that drives the modeling for humans without having a model itself. Since performing experimental studies by applying injected plutonium to humans is not conducted for obvious reasons, studies are instead conducted on rats and other mammals and their data extrapolated to humans in order to try to build the best model possible.

Obviously, there is a great number of radionuclides that humans can be exposed to whether they are from radioactive materials used in medicine, nuclear power plants, or fallout for example. However, there is limited human biokinetic data available on the exposure to these radionuclides. Animals have primarily been the source of biokinetic data that is used to develop the biokinetic models for humans. A vast amount of the data used for human modeling has been recorded in different scientific reports such as ICRP (1972, 1986, 1989, 1993, 2001) and NCRP (1993, 1998, 2001, 2006) as well as several other sources.

There are several reasons that using animals is beneficial in helping to build a human biokinetic model. The radionuclide, the amount of activity, and route of entry are all known when using animals for the experiment. This helps eliminate several variables that typically occur when using data from accidental human exposures. The experiment can also be conducted in a controlled environment where the only variables are the ones that are introduced. Obviously, this scenario would rarely occur with humans, but it does provide the information to help build a human biokinetic model.

The objective of this study is to build a rat systemic biokinetic model for  $^{239}\text{Pu}$ . Using the data provided from rats in a controlled environment and statistical methods for determining the best fit, a biokinetic model for rats will be established. The rat model used a simplified version of the human biokinetic model as defined in ICRP 67 as a starting point and then changed based on

the data and applied statistical method in order to determine the efficacy of each model. The structure of the model consisted of blood as a central compartment which is connected to the other compartments consisting of organs and soft tissues. These compartments in turn either recycled to the blood compartment or to excretion either through urine or feces. The goal of this model is that future research for human biokinetic models while using rats to help build this model will have a better method for building and understanding the correlation between the rat model and the human model.

## CHAPTER 2

### LITERATURE REVIEW

#### Plutonium

Plutonium is a radioactive element that is a heavy anthropogenic metallic element with atomic number 94 (Shleien et al. 1998). It was discovered in 1940 at the University of California by Seaborg et al. by bombarding Uranium with deuterons in a 60-inch cyclotron which resulted in the discovery of  $^{238}\text{Pu}$  (Seaborg et al. 1946). While plutonium was discovered in 1940, the results of its discovery was not published until 1946, after the end of World War II. This was at least in part to the discovery that  $^{239}\text{Pu}$  could fission and be used as an atomic bomb. The equation for the  $^{238}\text{Pu}$  reaction can be seen in equation 1.



Plutonium was named after Pluto, which was considered a planet at the time, following the discovery of Uranium named after Uranus and Neptunium named after Neptune. It is a silvery white metal part of the actinide series (Taylor 1973). It melts at 639.5 °C boils at 3,235 °C. It has a density of 19.84 g/cm<sup>3</sup> at room temperature.

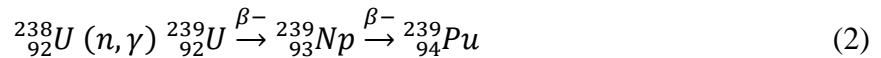
Since the discovery of  $^{238}\text{Pu}$ , there have been a total of 20 plutonium isotopes that have been characterized, not including those isotopes that are metastable. They range in mass number from 228 to 247. The most stable isotopes are  $^{244}\text{Pu}$ ,  $^{242}\text{Pu}$ , and  $^{239}\text{Pu}$  with half-lives of  $8.26 \times 10^7$  years,  $3.763 \times 10^5$  years, and 24,065 years respectively (Shleien et al. 1998). Only  $^{238}\text{Pu}$  and  $^{239}\text{Pu}$

have found widespread use either for military or peaceful applications (Taylor 1973). Table 1 shows the half-lives, decay modes, and radioactive decay properties of selected isotopes of plutonium.

**Table 1.** Half-life, decay modes, and radioactive decay products of selected plutonium isotopes (Shleien et al. 1998).

Nuclide	T <sub>1/2</sub>	Decay Mode	Decay Products and Frantional Yield			
			Nuclide	Fraction	Nuclide	Fraction
<sup>238</sup> Pu	87.74 y	Alpha, SF	<sup>234</sup> U	1 SF		1.84*10 <sup>-9</sup>
<sup>239</sup> Pu	24065 y	Alpha	<sup>235</sup> U	1		
<sup>240</sup> Pu	6537 y	Alpha, SF	<sup>236</sup> U	1 SF		4.95*10 <sup>-8</sup>
<sup>241</sup> Pu	14.4 y	Alpha, Beta	<sup>237</sup> U	2.45*10 <sup>-5</sup>	<sup>241</sup> Am	1
<sup>242</sup> Pu	3.763*10 <sup>5</sup> y	Alpha, SF	<sup>238</sup> U	1 SF		5.5*10 <sup>-6</sup>
<sup>243</sup> Pu	4.956 h	Beta	<sup>243</sup> Am	1		
<sup>244</sup> Pu	8.267*10 <sup>7</sup> y	Alpha, SF	<sup>240</sup> U	1 SF		1.25*10 <sup>-3</sup>

Plutonium is produced on a widespread scale in various nuclear reactors (Taylor 1973). Arguably the most important plutonium isotope is <sup>239</sup>Pu. It is a fissile element produced by irradiating <sup>238</sup>U with neutrons (Shleien et al. 1998). The production of <sup>239</sup>Pu can be described in the equation 2 below as:



The decay chain of <sup>239</sup>Pu has several branching fractions until it decays to stable <sup>207</sup>Pb. It decays almost exclusively by alpha decay with a couple exceptions. Table 2 shows the decay chain of <sup>239</sup>Pu to <sup>207</sup>Pb.

**Table 2.** Decay chain and branching fractions of  $^{239}\text{Pu}$  (ICRP 2008).

Nuclide	Halflife	Daughter Products			
		f1	Nuclide	f2	Nuclide
1 $^{239}\text{Pu}$	$2.411 \cdot 10^4$ y	$9.994 \cdot 10^{-1}$	$^{235\text{m}}\text{U}$	$6 \cdot 10^{-4}$	$^{235}\text{U}$
2 $^{235\text{m}}\text{U}$	26 m	1.00	$^{235}\text{U}$		
3 $^{235}\text{U}$	$7.04 \cdot 10^8$ y	1.00	$^{231}\text{Th}$		
4 $^{231}\text{Th}$	25.52 h	1.00	$^{231}\text{Pa}$		
5 $^{231}\text{Pa}$	$3.276 \cdot 10^4$ y	1.00	$^{227}\text{Ac}$		
6 $^{227}\text{Ac}$	21.772 y	$9.862 \cdot 10^{-1}$	$^{227}\text{Th}$	$1.38 \cdot 10^{-2}$	$^{223}\text{Fr}$
7 $^{227}\text{Th}$	18.68 d	1.00	$^{223}\text{Ra}$		
8 $^{223}\text{Fr}$	22.00 m	1.00	$^{223}\text{Ra}$	$6 \cdot 10^{-5}$	$^{219}\text{At}$
9 $^{223}\text{Ra}$	11.43 d	1.00	$^{219}\text{Rn}$		
10 $^{219}\text{Rn}$	3.96 s	1.00	$^{215}\text{Po}$		
11 $^{219}\text{At}$	56 s	$9.7 \cdot 10^{-1}$	$^{215}\text{Bi}$		
12 $^{215}\text{Bi}$	7.6 m	1.00	$^{215}\text{Po}$		
13 $^{215}\text{Po}$	$1.781 \cdot 10^3$ s	1.00	$^{211}\text{Pb}$		
14 $^{211}\text{Pb}$	36.1 m	1.00	$^{211}\text{Bi}$		
15 $^{211}\text{Bi}$	2.14 m	$9.972 \cdot 10^{-1}$	$^{207}\text{Tl}$	$2.76 \cdot 10^{-3}$	$^{211}\text{Po}$
16 $^{207}\text{Tl}$	4.77 m	1.00	$^{207}\text{Pb}^{\text{a}}$		
17 $^{211}\text{Po}$	0.516 s	1.00	$^{207}\text{Pb}^{\text{a}}$		

<sup>a</sup> stable nucleus

## Biokinetic Models

One of the first recommendations on plutonium were written in ICRP 2 (1959). The report detailed that data from human cases was used when possible, but a majority of the data was based on animal experiments. While a specific biokinetic model was not defined in the report, recommendations on the maximum permissible total body burden were given and identified the major organs of plutonium retention as the bone, liver, and kidney.

The next scientific report which offered updates on plutonium as well as other actinides was in ICRP 19 (1972). These revisions were made possible due to a great deal of more available

and widely conducted research. Studies on rats, mice, pigs, and dogs were all used in the report. The assumptions and information provided in this report were used in ICRP 30, including the models of the metabolism of plutonium in humans. While a great deal of the information in ICRP 30 is now obsolete due to revised dosimetry and dose limits in ICRP 60, the information on biokinetic data provides the basis for later reports. There are, however, shortfalls in the ICRP 30 model. The research conducted by Langham et al. was the primary resource estimating plutonium body burdens from urine (1980). In the years after the equations were developed, data indicated the possibility of large overestimates of body burdens for times greater than 5 years (Leggett 1985).

One of the first biokinetic models for plutonium was developed by Leggett (1985). It was developed to describe the retention, translocation, and excretion of plutonium from the blood of an adult human. The major benefit of this model over previous iterations was basing the model on physiological processes instead of simply calculations like the ones seen in ICRP 2 and ICRP 30. The model can be seen in Figure 1.

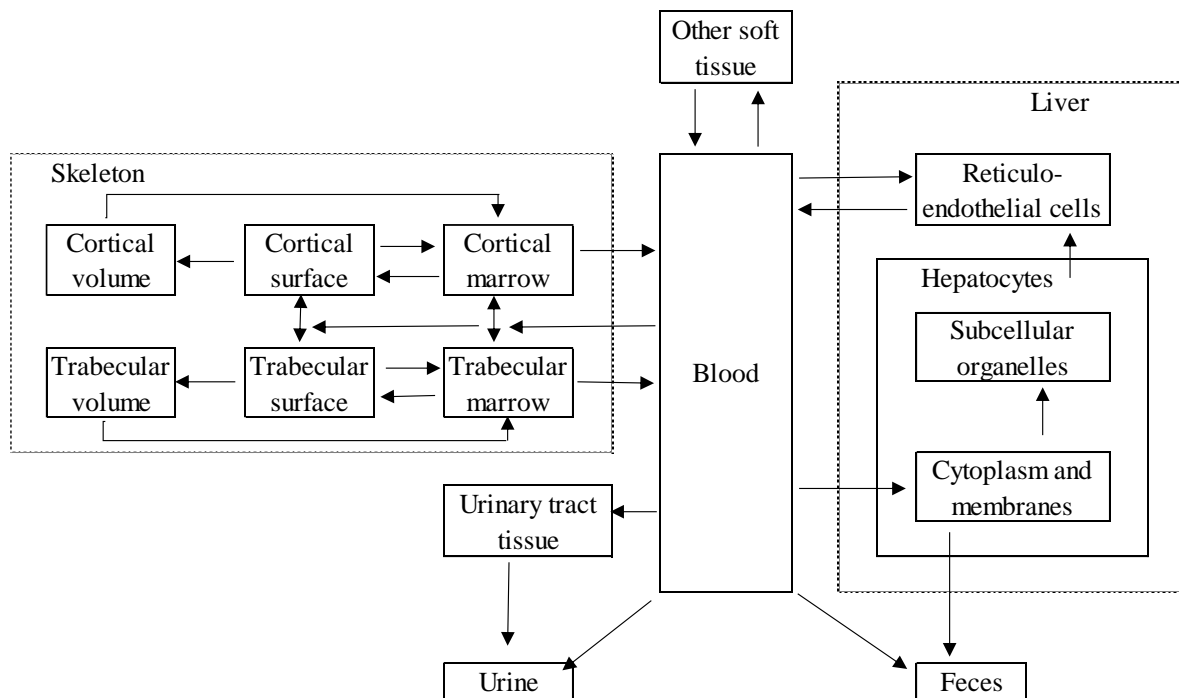


**Figure 1.** Compartments and directions of movement of Pu (Leggett 1985).

This model predicts the activity  $A(t)$  at time  $t$  in each compartment after contamination of the blood with plutonium at time 0. As can be seen in Figure 1, the model focuses on the primary organs known to have the highest plutonium deposition, the skeleton and the liver. The model divides the skeleton compartment into six compartments, allowing for the translocation of plutonium in the different cortical and trabecular areas of the bone. The model also allows for multiple compartments in the liver with blood flowing between multiple compartments. Leggett also recognized the retention of plutonium in the body varied with age and therefore made a provision for consideration of age in parameter values.

The Leggett 1985 model was adopted by ICRP 56 (1989). This report also used data and assumptions from ICRP 48 which confirmed the previous data that the skeleton and liver were the primary sites for deposition accounting for at least 80% of the plutonium reaching the blood. A majority of the data used to develop these models is based on animal studies (ICRP 1986). It is

assumed for this project that the deposition of plutonium among the cortical and trabecular bones was uniform and the retention in the gonads is permanent with 0.035% of plutonium deposited in the testes and 0.011% in the ovaries; a set of assumptions entirely consistent with ICRP 30.

The plutonium biokinetic model was updated in ICRP 67 to fit a more generic approach for bone seekers. This revision to Pu modeling was intended to improve estimates of dose to some radiosensitive organs, and to include new information on retention of plutonium in soft tissues and its excretion after recent injection (Leggett and Eckerman 1993). The model added age specific parameters for the skeleton and liver. It was assumed that for all ages after injection, the skeleton and liver will receive 80% of plutonium leaving the blood (ICRP 1993). For adults, the deposition of plutonium in the skeleton and liver is set as 5:3 ratio. For infants and 1-year old children, the ratio is 7:1. For ages 5 to 15 years, the ratio is 6:2. It is assumed that trabecular surfaces receive 60% of the plutonium deposition in the skeleton and cortical surfaces receive 40% for adults. All other ages are assumed to receive 50% of plutonium deposition on the trabecular surfaces and 50% on the cortical surfaces. Figure 2 shows the ICRP 67 biokinetic model. The transfer rates from each source to target organ can be seen in Table 3.

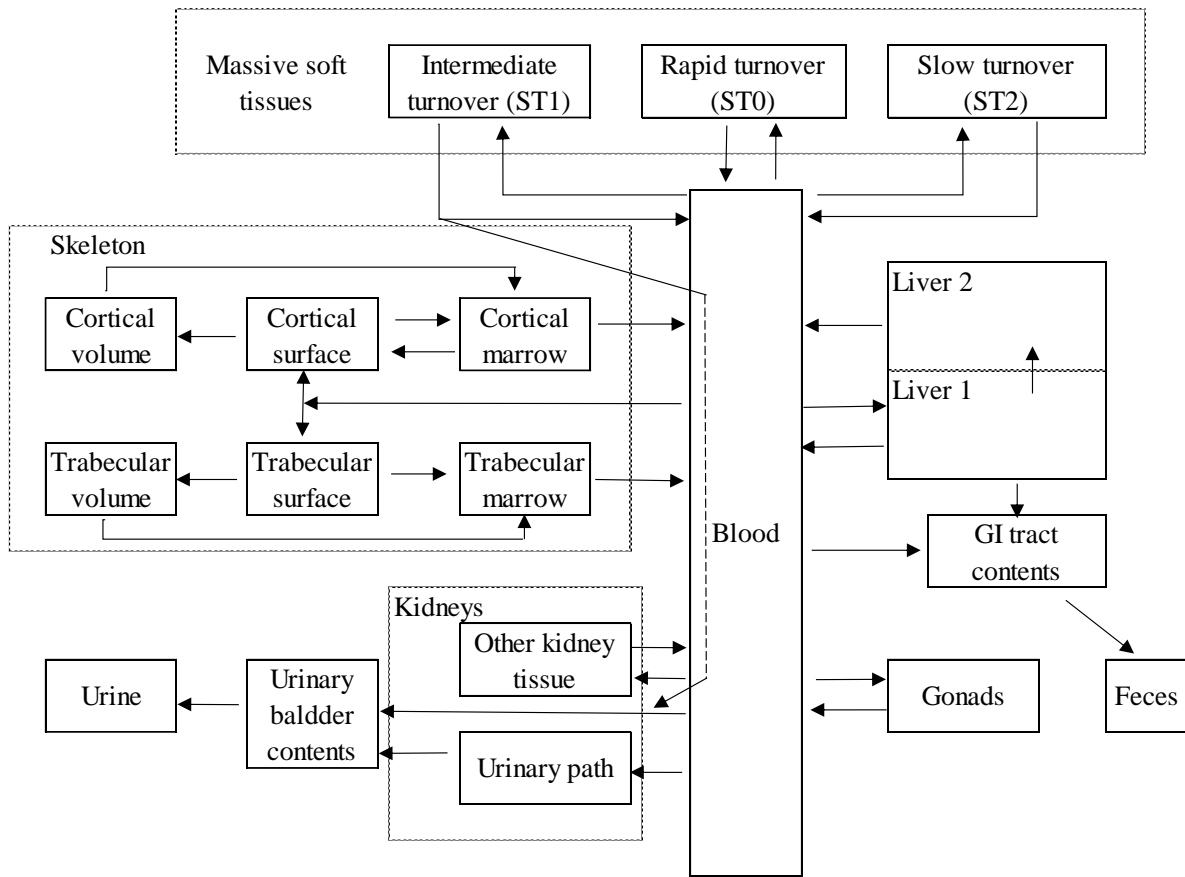


Figure 2. ICRP 67 biokinetic model (ICRP 1993).

**Table 3.** ICRP 67 transfer rates in adults for plutonium model (1993).

Source to Target Organ	Transfer rate (day <sup>-1</sup> )
Blood to Liver 1	0.1941
Blood to cortical surface	0.1294
Blood to trabecular surface	0.1941
Blood to urinary bladder content	0.0129
Blood to kidney (urinary path)	0.00647
Blood to other kidney tissue	0.00323
Blood to ULI contents	0.0129
Blood to testes	0.00023
Blood to ovaries	0.000071
Blood to ST0	0.2773
Blood to ST1	0.0806
Blood to ST2	0.0129
ST0 to blood	0.693
Kidneys (urinary path) to bladder	0.01386
Other kidney tissue to blood	0.00139
ST1 to blood	0.000475
ST1 to urinary bladder contents	0.000475
ST2 to blood	0.000019
Trabecular surface to volume	0.000247
Trabecular surface to marrow	0.000493
Cortical surface to volume	0.0000411
Cortical surface to marrow	0.0000821
Trabecular volume to marrow	0.000493
Cortical volume to marrow	0.0000821
Cort/trab bone marrow to blood	0.0076
Liver 1 to Liver 2	0.00177
Liver 1 to small intestine	0.000133
Liver 2 to blood	0.000211
Gonads to blood	0.00019

While the ICRP 67 model was improvement over the ICRP 56 model because it accomplished a number of pragmatic end points, such as taking into account the bladder since ICRP 60 had started to include the bladder as significant with respect to radiocarcinogens and introduced a weighting factor for the bladder, there were still limitations (Luciani and Polig 2000). After the release of the ICRP 67 biokinetic model, changes were proposed to address the

deficiencies of the model based on new research, data, and information. Two specific papers discussed the changes written by Luciani and Polig (2000) and Leggett et al. (2005).

Luciani and Polig proposed a revised plutonium biokinetic model in order to achieve a more realistic modeling of the excretion, specifically for long times after exposure (Luciani and Polig 2000). The new model was based primarily on the data collected from Langham et al. Changes to the skeleton compartments were in the ICRP 67 model were previously proposed by Polig (1997). These changes were adopted for the Luciani and Polig model with the addition of time dependent transfer rates for these compartments. The other recommended changes to the ICRP 67 model was the removal of the path between ST1 and the urinary bladder contents (Luciani and Polig 2000). The changes discussed to the ICRP 67 biokinetic model can be seen in Figure 3. The new transfer rates for the model can be seen in Table 4.

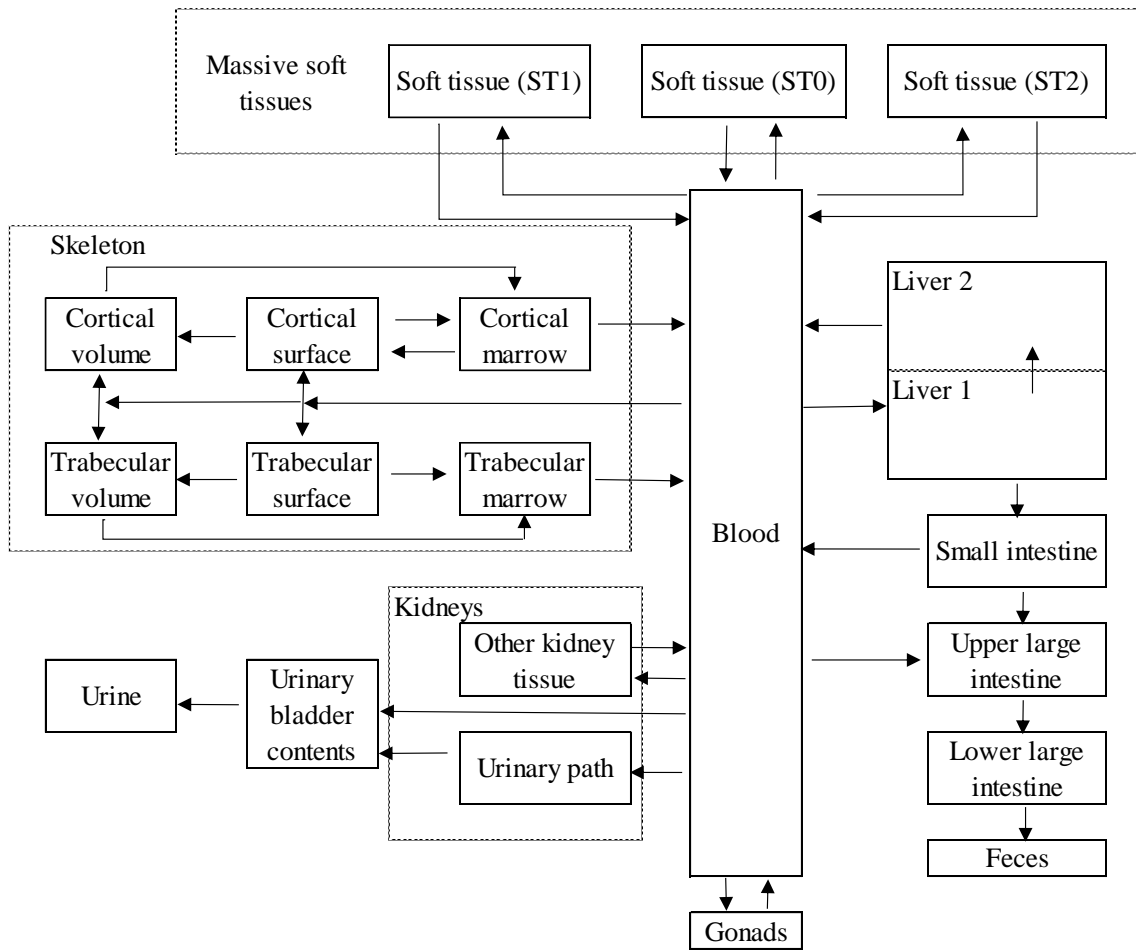


**Figure 3.** Optimized version of the ICRP 67 model for plutonium (Luciani and Polig 2000).

**Table 4.** Transfer rates of optimized plutonium biokinetic model in adults (Luciani and Polig 2000).

Source to Target Organ	Transfer rate (day <sup>-1</sup> )
Blood to Liver	0.120
Blood to cortical surface	0.0952
Blood to trabecular surface	0.226
Blood to cortical volume	0.0048
Blood to trabecular volume	0.0716
Blood to urinary bladder content	0.00946
Blood to urinary path	0.00992
Blood to other kidney tissue	0.00323
Blood to ULI contents	0.008
Blood to testes	0.00023
Blood to ST0	0.2773
Blood to ST1	0.0806
Blood to ST2	0.0129
ST0 to blood	0.139
Urinary path to urinary bladder content	0.0102
Urinary bladder content to excretion	12
Other kidney tissue to blood	0.00139
ST1 to blood	0.000950
ST2 to blood	0.000019
Trabecular surface to marrow	.00159 <sup>a</sup>
Trabecular volume to marrow	.00159 <sup>a</sup>
Cortical surface to marrow	.000156 <sup>a</sup>
Cortical volume to marrow	.0000822 <sup>a</sup>
Cortical marrow to blood	0.0076
Trabecular marrow to blood	0.0076
Liver 1 to Liver 2	0.01
Liver 1 to small intestine	0.0004
Liver 2 to blood	0.0004
Gonads to blood	0.00019
Small intestine to ULI	6.0
ULI to LLI	1.8
LLI to excretion (feces)	1.0

<sup>a</sup>Values up to 35 years of age. Double values at 60 y and linear interpolation between 35 and 60 y are assumed.

Leggett et al. proposed another model that differed from Luciani and Polig's model but still based off the ICRP 67 biokinetic model, with the exception of the removal of the path from ST1 to the urinary bladder contents which both models discussed. This model made several changes to the ICRP 67 model but made two major changes in adding two compartments which can be seen in Figure 4. These changes also affect the transfer coefficients derived from the deposition fractions, half-times, as well as additional assumptions made to the model. Table 5 lists the transfer coefficients from the source organ to the target organ based on this model.

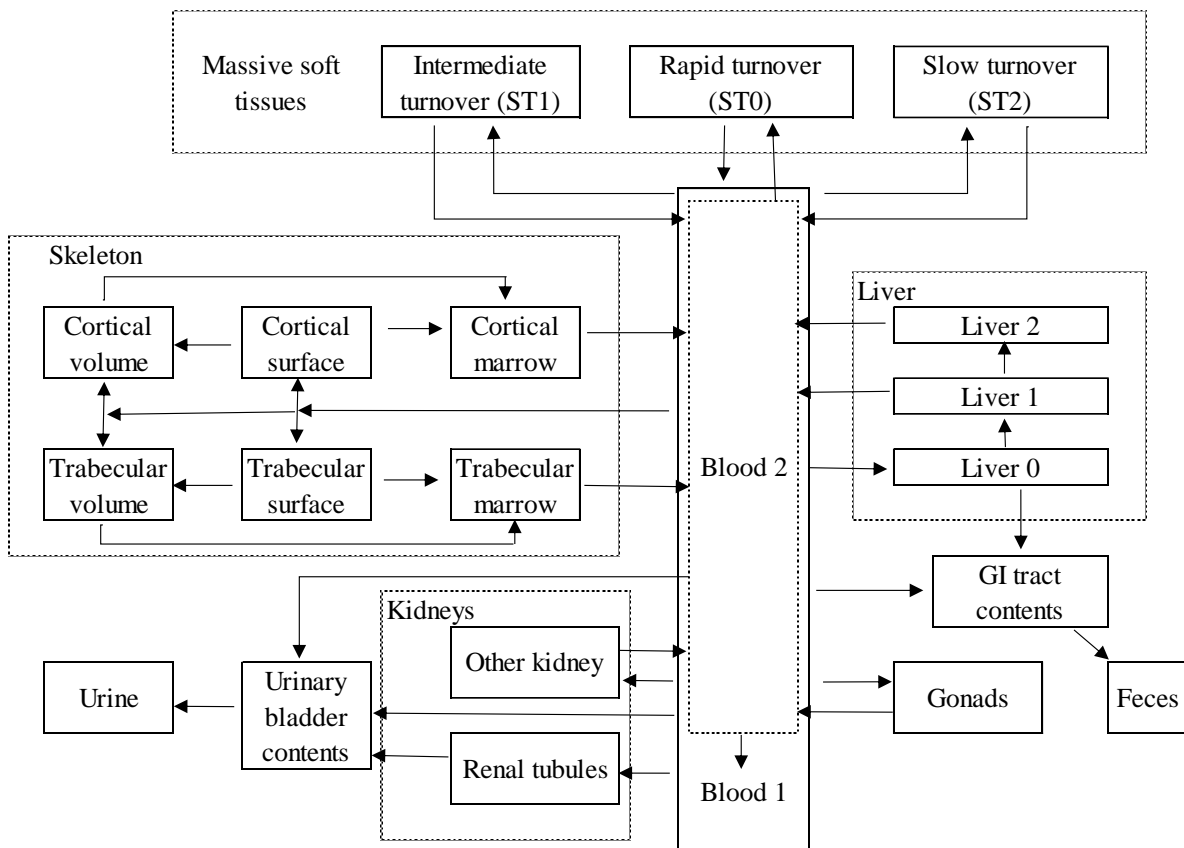


**Figure 4.** Structure of proposed model (Leggett et al. 2005).

**Table 5.** Baseline parameter values for a typical healthy adult (Legget et al. 2005)

Source to Target Organ	Transfer rate (day <sup>-1</sup> )
Blood 1 to liver 0	0.462
Blood 1 to cortical surface	0.08778
Blood 1 to cortical volume	0.00462
Blood 1 to trabecular surface	0.12474
Blood 1 to trabecular volume	0.01386
Blood 1 to urinary bladder contents	0.0154
Blood 1 to renal tubules	0.0077
Blood 1 to other kidney	0.000385
Blood 1 to ULI contents	0.01155
Blood 1 to testes	0.0002695
Blood 1 to ovaries	0.0000847
Blood 1 to ST1	0.018511
Blood 1 to ST2	0.0231
ST0 to blood 1	0.099
Blood 2 to urinary bladder contents	3.5
Blood 2 to blood 1	67.55
Blood 2 to ST0	28.95
Renal tubules to urinary bladder contents	0.017329
Other kidney to blood 2	0.0001266
ST1 to blood 2	0.001386
ST2 to blood 2	0.0001266
Liver 0 to small intestine contents	0.0009242
Liver 0 to liver 1	0.045286
Liver 1 to blood 2	0.00152
Liver 1 to liver 2	0.00038
Liver 2 to blood 2	0.0001266
Testes to blood 2	0.00038
Ovaries to blood 2	0.00038
Cortical surface to cortical marrow	0.0000821
Cortical surface to cortical volume	0.0000205
Cortical volume to cortical marrow	0.0000821
Trabecular surface to trabecular marrow	0.000493
Trabecular surface to trabecular volume	0.000123
Trabecular volume to trabecular marrow	0.000493
Cortical marrow to blood 2	0.0076
Trabecular marrow to blood 2	0.0076

Note. The initial input to blood by absorption or injection is assumed to distribute rapidly between Blood 1 (70%) and ST0 (30%).

The first was adding a second blood compartment, Blood 2, which resides entirely within the first blood compartment, Blood 1 (Leggett et al. 2005). Blood 2 receives all the recycled plutonium blood from the body and feeds the rapid turnover soft tissue compartment ST0, Blood 1, and the urinary bladder contents. The addition of Blood 2 implements the assumption that recycled plutonium has higher urinary clearance than the original input to the blood. Any portion of activity leaving Blood 2 that does not go directly to the urinary bladder contents is assumed to distribute in the same manner as the original input to blood.

The second compartment added to the ICRP 67 biokinetic model was a third liver compartment. Blood 1 flows to Liver 0 which is a rapid-turnover compartment (Leggett et al. 2005). Liver 0 feeds Liver 1 which is within the hepatocytes with intermediate-term retention. A small portion of the activity in Liver 0 is lost to bile. Most of the activity from Liver 1 is lost to Blood 2 while a portion enters the reticuloendothelial cells, Liver 2, which is then lost to Blood 2.

#### Animal Studies

As previously mentioned, the majority of information used for humans from radioactive materials such as health effects, biokinetic models, and amount of deposited materials comes from the experimentation of animals. This information has been repeatedly used in the scientific community whether it be in the form of committees or reports such as those that have been distributed by ICRP, NCRP, and others.

While a great amount of research on plutonium has come from studies on rats such as those conducted by Carritt et al. 1947, Scott et al. 1948, Taylor 1962, Turner and Taylor 1968, Durbin et al. 1972, Morin et al. 1972, Stather and Howden 1975, Durbin 1975, Taylor 1977, Sontag 1981, Stanley et al. 1982, Taylor 1973, and Talbot et al. 1990, there have also been experimental studies

conducted on other mammals to help understand the distribution of plutonium. These include studies conducted on mice (Austin et al. 1999, Austin and Lord 2000), beagles (Lloyd et al. 1978, Dagle et al. 1983, Polig 1989, Lloyd et al. 1997, Polig et al. 2000), rabbits (Rosenthal et al. 1972), and nonhuman primates (Stanley et al. 1982, Durbin et al. 1985, Poudel et al. 2016). Several of these studies offer comparisons to multiple animals. This is by no means an all-encompassing list of the research conducted on animals but highlights some of the work that has been conducted.

One of the earliest studies examining the administration of plutonium through IV injections in rats was conducted by Carritt et al. (1947). This study was conducted shortly after the end of World War II but several years after the discovery of plutonium. The goal of the study was examining body distribution and excretion of plutonium using different solutions. While there were some differences in the excretion of feces to urine ratio after the first day among the different solutions, by the thirtieth day, the ratios were essentially the same for all the solutions with an average ratio of 16 to 1. This helps in supporting a conclusion that the solution used for injection is not necessarily of concern after longer periods of time when it comes to plutonium excretion but does show the high levels of plutonium in fecal matter. The data also showed that regardless of the plutonium solution, the skeleton was a major source of deposition, followed by the liver, although the percent of injected dose did vary somewhat amongst the solutions. The percent of injected dose recovered for the kidneys and spleen were by far lower than the recovery for the skeleton and liver. This high deposition of plutonium in the skeleton and liver concurs with multiple experimental studies.

A study conducted by Scott et al. looked at the metabolism of plutonium in the rat through intramuscular injection (1948). While the route of injection differed, the skeleton was by far had the greatest deposition of plutonium, followed by the liver. This study was conducted over the

period of 256 days. Of note is the deposition of plutonium in the rat was the same at 8 days as it was at 256 days indicating there was no redistribution of plutonium in the adult rat after its initial deposition.

Perhaps the most interesting research on plutonium experimental studies has been those conducted by Durbin at Lawrence Berkley Laboratory. The first of these studies was conducted by Durbin et al. and examined the data from several previous studies but ultimately used the data from Shubert et al. in 1950, although several estimates from the other data sets were used. Using this data, a conventional kinetic model for the rat was introduced to describe the transport and deposition of IV injected plutonium which can be seen in Figure 5 (1972).

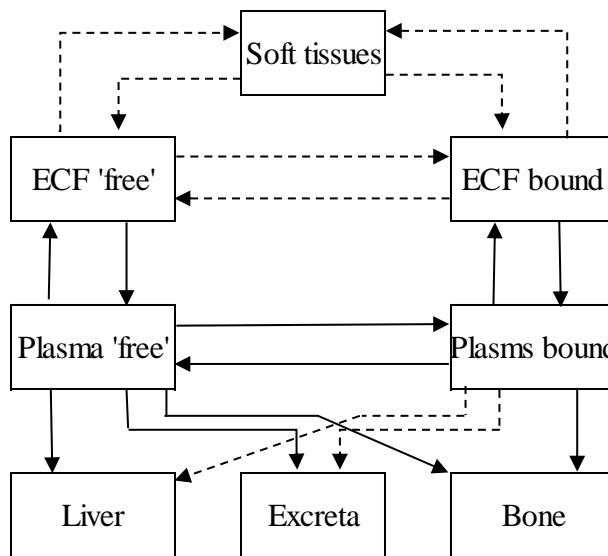


**Figure 5.** Compartment model of Pu transport and uptake in tissues of the rat 0.25-18 hr after IV injection of  $^{239}\text{Pu(IV)}$  citrate (Durbin et al. 1972).

As can be seen, the blood compartment is broken down into two extracellular fluid (ECF) compartments and two plasma compartments. This was done in part by using *a priori* assumptions. As seen in previous studies, plutonium is primarily deposited in the skeleton, bone, and excretion.

While there is no recycling from excretion, there is from the skeleton and the liver which is not shown in this model. This is due to the model being restricted to the first 0.25 to 18 hours in which no feedback was seen, eliminating the need for these calculations. The transfer rates that were calculated between the compartments are those that provided the best fit of the Schubert et al. data. It should also be noted that the paths that are marked as dashed arrows are where there is no transfer between the compartments. While the limited amount of time that is used may be a limitation of the model, it was a guide for subsequent research.

The second research conducted by Durbin again examined previous research conducted but looked at the results of both multiple different animals and multiple routes of plutonium administration (1975). Consistent with previous studies, across all mammals examined in these studies, plutonium primarily deposits in the skeleton and the liver. Of interesting note is the skeleton of the rat when the animal is injected with plutonium. The research shows that when compared to the skeleton of a dog, the rat skeleton accumulates a larger fraction of plutonium. This may be due to the adult rat skeleton never fully maturing during the laboratory time frame.

The differences between animals and humans offer a caution when applying animal research to human modeling with the knowledge that more experimental studies with humans are ethically undesirable. The assumption that metabolic parameters developed from a study of adult animals can adequately describe the how the radionuclide will behave in adult humans may be an oversimplification, especially when applying these models to humans of different ages and sex (Durbin 1975). The older plutonium model on rats indicates the need for an updated version based on new data and information not readily available during previously conducted studies.

## Akaike's Information Criterion (AIC)

Selecting the appropriate statistical method for modeling is an important issue for any data analysis (Pan 2001). When determining which statistical method is best to be used in predicting the best fit in modeling of data, several options are available. Even among a specific statistical method, there are several different breakdowns that can be used. For example, if using a Chi-squared distribution for the statistical method, there are options of using a Student's t-test derived from Chi-squared distribution. The Chi-square distribution itself is a special case of the gamma distribution. This can provide a great many options when trying to decide which statistical model should be used.

The complexity of a model is a part of analyses. There are basically two methods of thinking when it comes to the complexity of the model. Some scientists believe more complex models are more desirable while others prefer a model that emphasizes parsimony (Aho et al. 2014). As stated in Aho et al. 2014, a parsimony model is one that is able to “balance uncertainty, caused by excessively complex models, and bias, resulting from overly simplistic models.”

Akaike's Information Criterion (AIC) was introduced during 1973 (deLeeuw 1992). It is based on the likelihood and asymptotic properties of the maximum likelihood estimator (MLE) (Pan 2001). It has a close connection to the maximum likelihood method (deLeeuw 1992). AIC is an example of a parsimony statistical method (Aho et al. 2014). Equation 3 provides an expression for AIC parameters,

$$AIC = (-2) \log (\text{maximum likelihood}) + 2k \quad (3)$$

where  $k$  is the number of independently adjusted parameters (Akaike 1974).

When determining the goodness of fit using AIC, the ideal model is the one that minimizes the AIC value. It can therefore be shown that AIC rewards goodness of fit. However, AIC also introduces a penalty when introducing more complexities into the model. Introducing more parameters to the model usually improves the goodness of fit, but also increases the complexity of the model. AIC discourages overfitting and thus is the reason for the penalty. AIC is most effectively applied when determining the decision for the final estimate of a finite parameter model when several estimates are acquired corresponding to the restrictions of the model (Akaike 1973). The balance of determining the preferred model is one that introduces enough parameters for improving the goodness of fit without increasing complexities in order to produce a minimum AIC value.

## CHAPTER 3

### DATA

#### Animals and Animal Care

The collection of data was performed at Lovelace Respiratory Research Institute (LRRRI). A total of 48 F344 rats from Charles River Inc. These rats were 11 weeks old at time of injection. The rats were randomly divided into 8 groups, with each group consisting of 3 males and 3 females. Each group of rats was randomly assigned to a sacrifice time of either 1 hour, 4 hours, 1 day, 2 days, 4 days, 8 days, 16 days, or 28 days (Weber 2019).

Upon receipt of the rats, each were jugular vein cannulated (JVC) animals in which a sterile polyethylene catheter was implanted surgically into the jugular vein. The JVC access port was sealed with a sterilized stainless-steel pin. A patency check was conducted for each port using a sterile technique. In order to prevent coagulation and plugging, after the patency check, a heparinized dextrose solution was placed in the lumen of the cannula.

The rats were quarantined and acclimated in metabolism cages for 1 week. Each rat had access to food and water. Food was refreshed on a daily basis and water bottles were refilled as necessary and changed every week. The food was analyzed for contaminants by the manufacturer and was used at LRRRI within the stated shelf life. Municipal water was given to the rats which is the standard used at LRRRI for animal studies. The staff at LRRRI observed the rats twice daily for morbidity and mortality.

## Experimental Study

For the study, each rat received a single bolus intravenous (IV) injection of 190.7 nCi ( $7.0559 \times 10^3$  Bq) of  $^{239}\text{Pu}$ -citrate in a 200- $\mu\text{L}$  formulation via the IV port. After injection, the syringe was flushed with saline to ensure the entire formulation was received by the rat.

The rats were placed in individual metabolism cages where urine and fecal samples were collected on a daily basis except in the cases of the rats who were sacrificed before providing a sample. A cage rinse was conducted every third day and combined with the urine and fecal samples for radiochemical processing and to measure the  $^{239}\text{Pu}$  content.

Each group of rats were euthanized at the selected time they were assigned at the beginning of the experiment. They were injected with Euthasol together with pneumothorax. After the rat was sacrificed, a blood sample was collected. Each rat was then dissected and the tissues and organs were separated in order to determine the amount of radioactivity in each one. The tissues and organs were the liver, spleen, kidneys, lungs, muscle (quadriceps), bone (femur), GI tract, gonads, pelt, and remaining soft tissues which primarily consisted of muscle and connective tissue.

## Radioanalysis

The tissue and organ samples were placed in the appropriately sized beakers and assayed for  $^{239}\text{Pu}$ . Smaller tissues were placed in 50-mL beakers and larger samples were placed in 250 mL beakers. This included the urine and fecal samples. The samples were dried at 95°C for 24 hours. They were then ashed at 550°C for 72 hours. The ashed samples were treated with  $\text{HNO}_3$  and a few drops of 30%  $\text{H}_2\text{O}_2$  on hot plates and taken to dryness. The samples were then remuffled for 24 hours at 550°C. The ashed sample process was repeated once more with the sampled being remuffled for 8 hours.

The samples were transferred to Teflon beakers and treated with 6M HF in concentrated HNO<sub>3</sub> and dried. Samples were then dissolved in 2M HNO<sub>3</sub> and aliquoted for counting on a liquid scintillation counter (LSC) with a scintillation cocktail. Spikes and blanks were also counted with the samples as part of the quality control (QC) process to determine the performance of the LSC.

#### Material Balance

The total recovered <sup>239</sup>Pu was determined by summing all of the radioactive results measurements for tissues, urine, feces, and cage wash samples. The material balance results are summarized in Table 6 by study group, sacrifice time, and the average fraction of <sup>239</sup>Pu recovered, as well as the study average of all of the groups. The study average was 84.5 ± 7.7%. The averages from each group were not as consistent as would have been liked. However, the results are deemed acceptable for the study.

**Table 6.** <sup>239</sup>Pu Material Balance Recoveries for the Experimental Groups in this Study

Study Group ID	Sacrifice Time (d)	Average Fraction Recovered (% , ± SD)
F	0.042	76.4 (5.8)
E	0.167	95.7 (3.9)
D	1	82.4 (5.0)
G	2	73.4 (7.6)
C	4	81.6 (13.8)
H	8	88.0 (5.8)
B	16	92.8 (9.2)
A	28	85.9 (10.5)
Study Average (% , ± SD)		84.5 (7.7)

## CHAPTER 4

### MATERIALS AND METHODS

#### Rat Model

The data from the tissues, organs, urine, and feces for each of the rats were entered in a modeling software program. To determine the fit of the model, AIC was used as the statistical method in order to assess the efficacy of the model. Depending on how the model fits based on the statistical methods, a new model was built, the rat data was run through the model again, and the statistical method was used to determine the fit of the new model. This iterative process was repeated until a model that yielded a minimum AIC value could be determined or it was presumed that the data at that time presented an issue with building a rat model.

The first model that was used can be seen in Figure 6. The model consists of each of the tissues, organs, urine, and feces that data was collected on during the experimental study, as well as their transport to and from the blood. As previously stated, once the model was run through the software to analyze the data from experiment, and AIC value was calculated to determine the fit of the model.

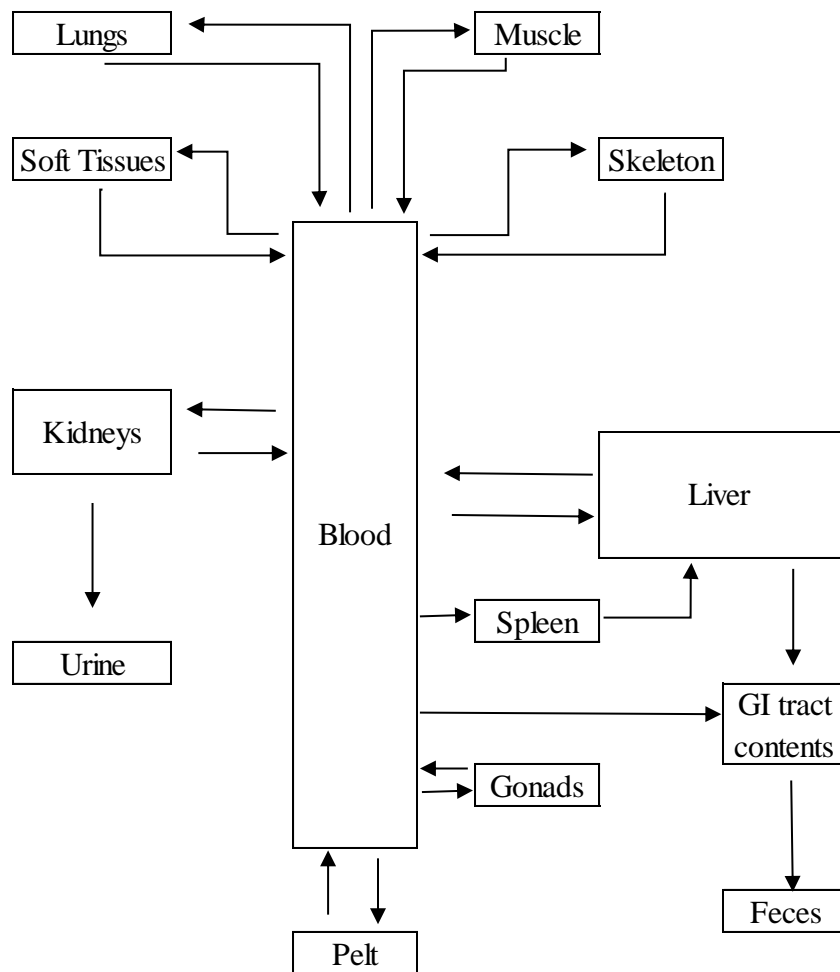


**Figure 6.** The initial model used to assess the fit of the data.

Since it was not expected that the first model would be an ideal rat model and multiple iterations would need to be conducted, the second model started to reduce the number of compartments and an example can be seen in Figure 7. The model focused on combining multiple organs and tissues into one compartment in order to reduce the number of complexities in the model. The reason behind reducing the number of compartments is the theory of this project that a simpler model would better explain the transport of  $^{239}\text{Pu}$  in the rat. Again, the statistical method was used to determine the efficacy of it and was further changed based on the results.

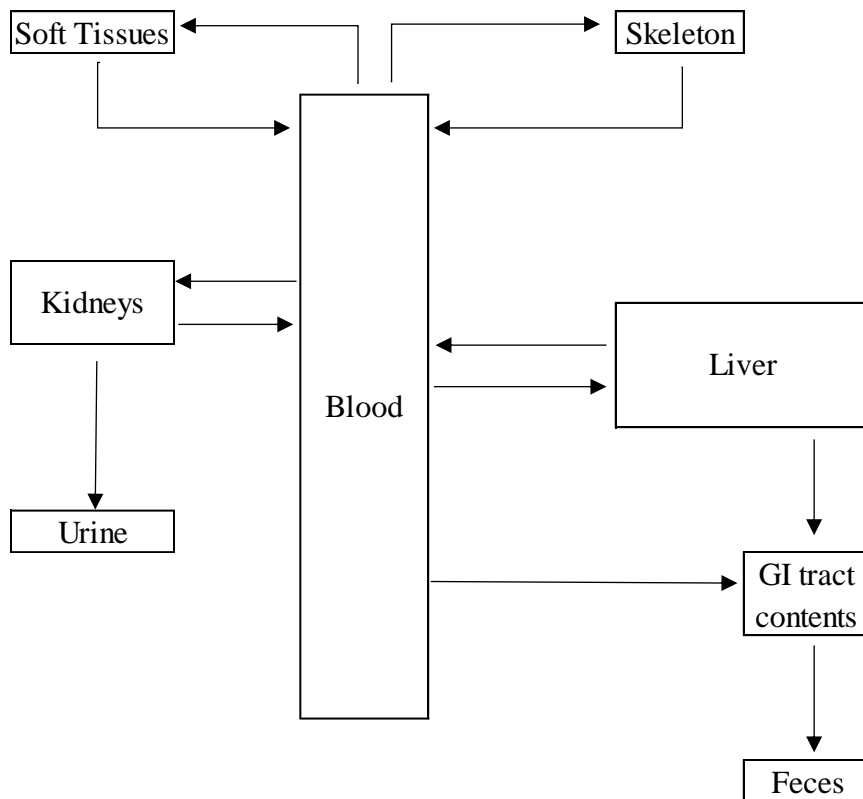


**Figure 7.** Simplified version of the rat model.

After assessing the fit of the reduced model, complexities were added back into the model as can be seen in Figure 8. Multiple models were constructed with different complexities added. The process of running the data through multiple models helped to determine which compartment needed additional information so a rat model that defined the transport of plutonium could be produced. In this case, the liver compartment was divided into two compartments, and the kidneys compartment had an additional section for a urinary path. This model is similar to the ICRP 67 biokinetic model with a few simplicities such as the skeleton only being one compartment instead of the six compartments seen in the ICRP 67 model.

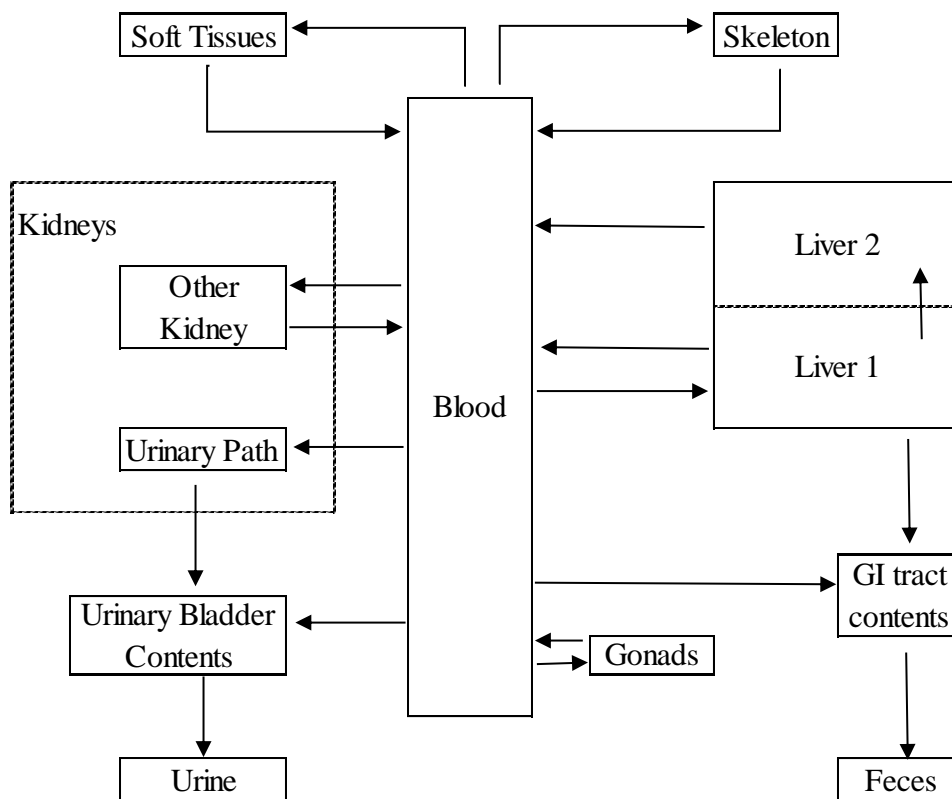


**Figure 8.** Complexities introduced to the rat model.

Adding further complexities to the model consisted of separating the tissue and organ compartments so that each has a separate compartment with their own transport between the blood or excretion. An example of this type of model can be seen in Figure 9. The soft tissue compartment now consists of only those soft tissues that data was originally collected for during the experimental study. The model still consists of multiple compartments for the liver and kidneys.

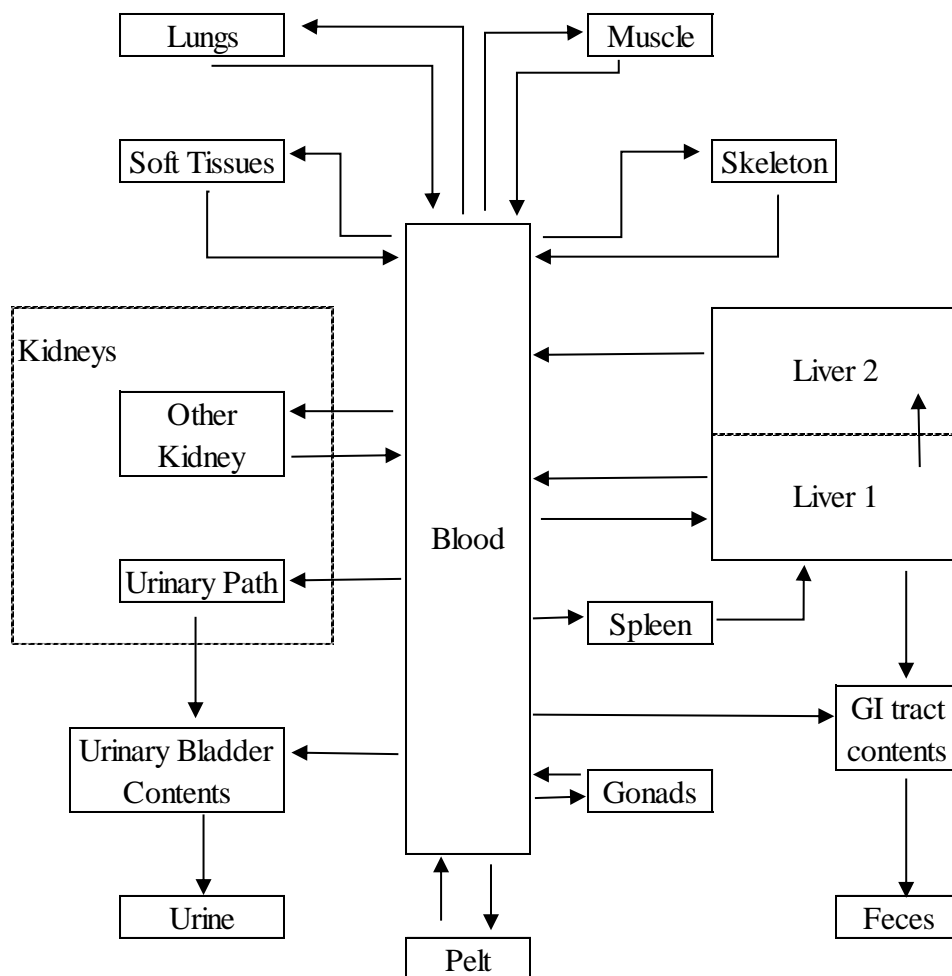


**Figure 9.** Further compartments added to the rat model.

## Modeling Software

The modeling software used for this project was SAAM II which allows the user to build compartmental models. SAAM II was developed by The Epsilon Group (TEG) which is a modeling, analytics, and simulation services company (TEG 2017). The user can build a proposed model, enter the relative data into the software, and have simulations conducted based on defined parameters and statistical method algorithms. Based on the results of the model, the user can easily change the parameters and have model run through the simulations again.

SAAM II uses an optimizer to fit the model to the data. It then runs through a series of iterations and adjusts the value of the adjustable parameters to obtain a best fit between the calculated values and the data. SAAM II has a convergence criteria which is an internal measure of the goodness of fit. The iterative process continues adjusting the parameters until the convergence criteria are satisfied or until the maximum number of iterations specified has been reached.

SAAM II was used to build several different compartmental models in order to determine the number of compartments and transfer rates for each compartment required to build a  $^{239}\text{Pu}$  systemic biokinetic rat model. To start, a compartment model similar to the ICRP 67 biokinetic model was used. The data was entered into SAAM II and processed to determine how the data fits the model. At this point, the number of compartments was reduced, such as folding the lungs and muscle into the soft tissue compartment. This new model was processed in SAAM II to determine how the data fits to a less complex model. Based on the results of this reduced model, further compartment reductions were completed. If the reduced model showed the data did not fit, the previous model was used, and different compartment reductions were completed.

Once a reduced compartment model was shown to fit the data, complexities to the model were added back to the model in order to ensure the best  $^{239}\text{Pu}$  systemic biokinetic model for rats had been determined. One example of these complexities is adding multiple compartments for the liver. Again, the models were processed to discover if these added complexities provided a better fit of the data than the reduced compartment model. This process was repeated as necessary until the best fit of the data was found.

## Statistical Method

The statistical method used for this study was Akaike's Information Criterion (AIC). It is based on the likelihood and asymptotic properties of the maximum likelihood estimator (Pan 2001). AIC is able to assess the quality of each of the rat models which provided the means for model selection.

After the initial model was built in the modeling software, AIC was used to check the quality of this model. As previously stated, the model then began to reduce the number of complexities. AIC was again used to assess the model during each compartment that was combined with the existing soft tissue compartment. If AIC determined this new model was a better quality than the previous model, another complexity was subtracted. However, if the opposite was true, the previous model was used again, and a different complexity was examined to see if it produced a better quality model.

The practice of reducing complexities in the model continued until AIC determined it had the highest quality model. At this point, complexities began to be reintroduced to the model, such as multiple compartments for the liver, to determine if this further improved the quality of the model. Again, the process of adding complexities continued until AIC determined the best quality rat model had been determined.

When determining the quality of each model using AIC, it is important to note that the equation SAAM II uses for AIC is slightly different than that in the literature and can be seen in equation 4,

$$AIC_{SAAM} = \frac{L + N_p}{M} \quad (4)$$

where  $L$  is defined as,

$$L = \left(\frac{M}{2}\right) (R(p) + \ln(2\pi)) \quad (5)$$

where  $R(p)$  is the objective function,  $N_p$  is the number of adjustable parameters in the model, and  $M$  is the total number of data points. Essentially to find the AIC value as defined in the literature, the reported AIC value listed in the statistics table of SAAM II needs to be multiplied by  $2M$ .

In order to determine which model has the highest quality,  $\Delta AIC$  was used and is defined in equation 6 as,

$$\Delta AIC = AIC_i - AIC_{min} \quad (6)$$

where  $AIC_i$  is the model being tested and  $AIC_{min}$  is the model who has the lowest calculated AIC value (Burnham and Anderson 2002). As a rule of thumb, if the  $\Delta AIC$  equals 0-2, then the model is considered to have substantial support and be a quality model. If  $\Delta AIC$  equals 4-7, then there is considerably less support for the model. If  $\Delta AIC$  equals 10 or greater, then there is essentially no support for the model.

## Hypothesis

H<sub>0</sub>: A simpler systemic biokinetic model will provide the best fit for the rat model.

H<sub>A</sub>: A simpler systemic biokinetic model will not provide the best fit for the rat model.

It is believed that not having as many complexities will theoretically show the importance of <sup>239</sup>Pu in the liver and skeleton since these are the dominant organs of transport. Less complexities will help allow for a better balance of the model between introducing enough parameters and improving the goodness of fit in order to find the balance necessary for a minimum AIC value. It is possible that in the end, the ICRP 67 biokinetic model or a model fairly similar to

it, such as the Leggett et al. (2005) or Luciani and Polig (2000) models, will be the model that best explains the transport of  $^{239}\text{Pu}$  through the rat. Conducting multiple iterations of the model will help determine the efficacy of each and ultimately decide whether the hypothesis or null hypothesis best represents the transport of  $^{239}\text{Pu}$  through the rat.

## CHAPTER 5

### RESULTS

Multiple models and iterations of these models were developed in order to try and create a  $^{239}\text{Pu}$  systemic model for rats. In total, 16 unique models were developed. Creating different iterations of these models consisted of adjusting pathways, either by changing the source to target compartment, adding new pathways that weren't originally inputted into the model, or deleting pathways. It is unknown exactly how many iterations of models were developed since several developed models were not able to determine a result and therefore multiple changes were made in order to try and produce one, such as changing pathways. For the sake of space, 3 unique model results are discussed that are considered to be the best examples of this research. Several other models that failed can be examined in Appendix A.

It should be noted that for the excretion compartments, the data was entered into SAAM II in a different manner than the other samples. While conducting trial runs of the models, it was noticed that the urine and feces compartments were unable to determine a proper fit of the sample data. Upon further investigation, it was determined that because there was no pathway leading away from either of these compartments, they were accumulating all the activity without a loss. A change was made to the data to reflect this by summing the data points for each rat to their previous sample. This resulted in a fit of the data and was used for all model construction. The only other edits made to the sample data were those that had an activity that was either zero or negative.

SAAM II is unable to process any data points that are not positive and therefore any data points that were zero or negative were excluded.

### First Compartmental Model

The first model that was constructed consisted of using all the data as separate compartments with the exception of the testes and ovaries which were combined into one gonads compartment due to the limited amount of data of each. Figure 10 shows the construct of the model in SAAM II with the pathways between the compartments designated as  $k(\text{target}, \text{source})$ . For example, the pathway from blood to the liver is designated as  $k(3,1)$ .

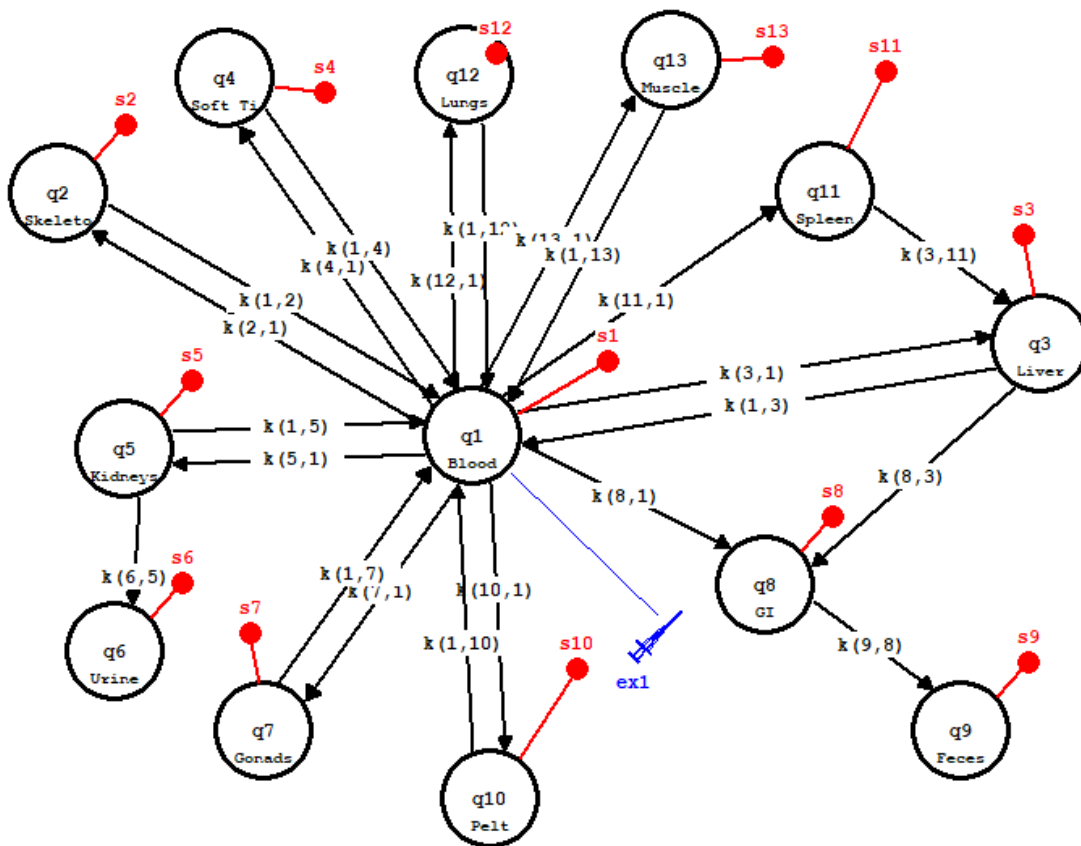


**Figure 10.** First model constructed in SAAM II. The red circles indicate the sample data associated with each compartment. The blue syringe indicates an injection into the blood compartment. The q1, q2, etc. designation in each compartment is how SAAM II represents the compartment.

Each of the compartments show recycling occurring back to the blood compartment apart from the spleen, GI, urine, and feces compartments. The data for each compartment was entered into SAAM II. Initial parameters with upper and lower limits were also entered based on the ICRP 67 transfer rates. For those pathways in which no transfer rates were included in ICRP 67, a parameter was entered based on an expected transfer rate to occur between the two compartments.

After all of the data and parameters were entered into SAAM II, a fit was run on the model. The first run on this model failed to converge. Multiple changes to the parameters had to be entered in order to get a result. The model processed the inputted data and once it was finally able to converge and calculated the parameters and AIC, but also concluded the covariance matrix was unreliable. This means as the data is not informative enough to allow reliable estimation of the parameters. Typically, the best fix for this issue is to collect more data or simplify the model. The parameters calculated by SAAM II are in Table 7.

**Table 7.** Parameters for first model construction.

Source to Target Organ	Transfer rate (day <sup>-1</sup> )
Skeleton to Blood	0.453
Liver to Blood	0.816
Soft tissue to Blood	15.840
Kidneys to Blood	0.951
Gonads to Blood	52.356
Pelt to Blood	0.134
Lungs to Blood	1.333
Muscle to Blood	20.162
Blood to Skeleton	777.636
Blood to Liver	-63.449
Spleen to Liver	44.229
Blood to Soft tissue	103.176
Blood to Kidneys	21.337
Kidneys to Urine	0.232
Blood to Gonads	164.631
Blood to GI	3.051
Liver to GI	1.803
GI to Feces	0.911
Blood to Pelt	8.322
Blood to Spleen	91.514
Blood to Lungs	10.567
Blood to Muscle	1676.387

The AIC/M value calculated by SAAM II is 6.001. The total number of data points  $M$  for this model was 1,250. As defined in the literature, this equates to an AIC value of 15,002.5.

Each of the samples are shown graphically in a semilog plot. The graphs show the amount of activity in Bq versus the time after injection in days. A fit of the data as calculated by SAAM II for each sample based on the parameters of the compartments is also shown. The results for the compartments are listed on a tissue by tissue basis.

A plot of the blood sample can be seen in Figure 11. The fit of the plot does not align well with the early data points up to day 8. The later data points seem to fit the plot better than the early time period.

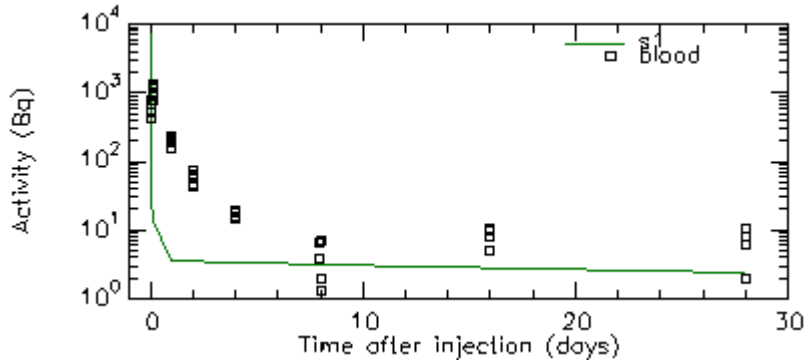


**Figure 11.** Semilog plot of blood sample in first constructed model.

A plot of the skeleton sample can be seen in Figure 12. The look of the curve itself does seem to at least mirror the data in that it starts with a steep incline and then gradually drops off over time. However, the fit is overestimating the data at all time periods.

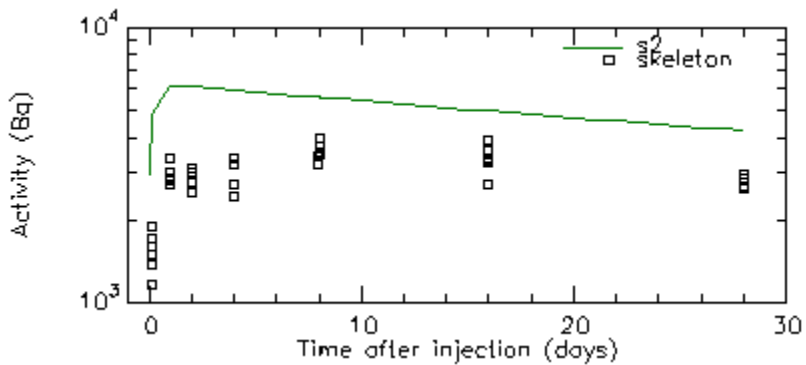


**Figure 12.** Semilog plot of skeleton sample in first constructed model.

A plot of the liver sample can be seen in Figure 13. Similar to the skeleton compartment in the look of the curve seems to follow the trend of the data points. In this case however, the fit is underestimating the data points with the exception of the data at time 0.04167 days.

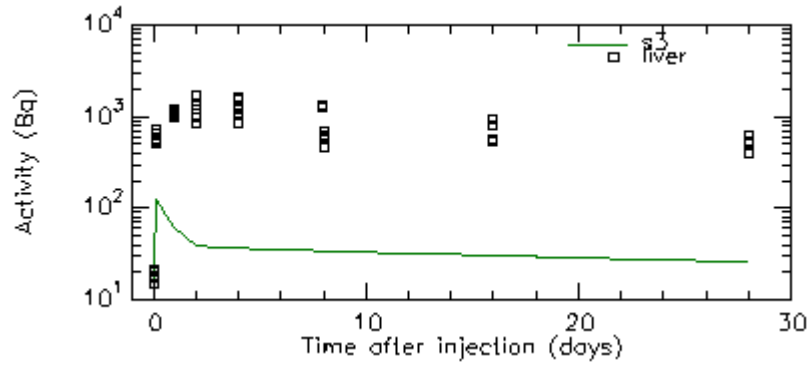


**Figure 13.** Semilog plot of liver sample in first constructed model.

A plot of the soft tissue sample can be seen in Figure 14. The fit does not quite align with the earliest data points and when it drops off it underestimates the rest of the data. The fit itself again does follow the relative trend of the data.

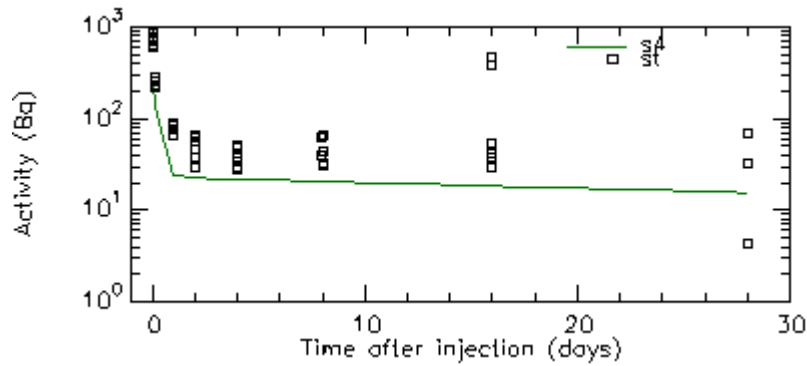


**Figure 14.** Semilog plot of soft tissue sample in first constructed model.

A plot of the kidneys sample can be seen in Figure 15. The fit of curve aligns fairly well with the early data points. The curve does start to fall off slightly faster than the data does and begins to underestimate the data during the later time periods.

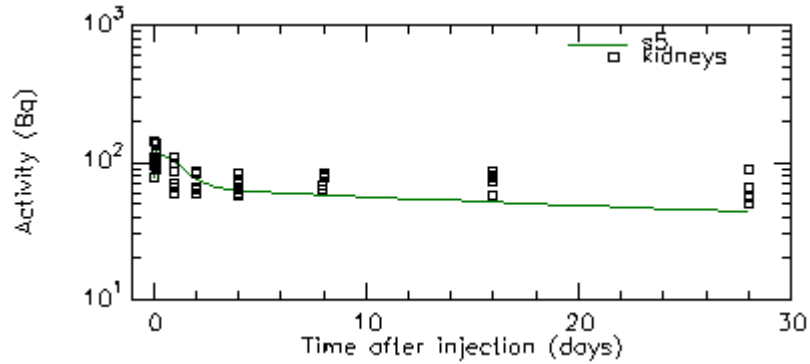


**Figure 15.** Semilog plot of kidneys sample in first constructed model.

A plot of the urine sample can be seen in Figure 16. The fit of the curve starts out underestimating the data points but does fit relatively well towards the later time periods. Part of this could be due to a lower data point during the first time period. It is possible that the fit would be even better if this data point was ignored since it is quite a bit lower than the other data points during the same time period.

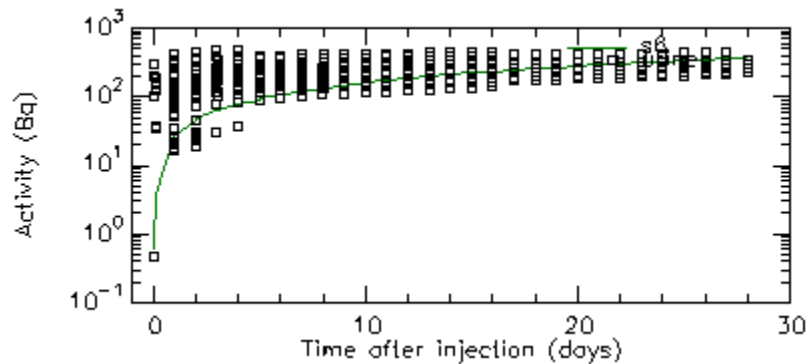


**Figure 16.** Semilog plot of urine sample in first constructed model.

A plot of the gonads sample can be seen in Figure 17. The curve fits the data relatively well. It does seem to trend towards the lower data points throughout the entire time period but does not either over or underestimate all of the data at any time period.

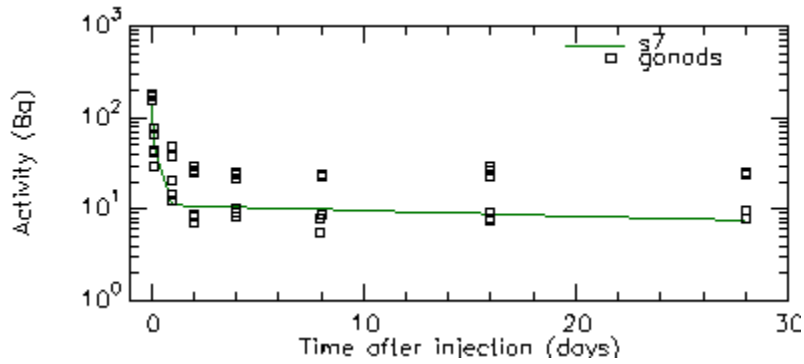


**Figure 17.** Semilog plot of gonads sample in first constructed model.

A plot of the GI sample can be seen in Figure 18. The curve starts by underestimating the fit of the data and does not reach the activity levels of some of the earliest data points. It does however fit with the remaining data points quite well.

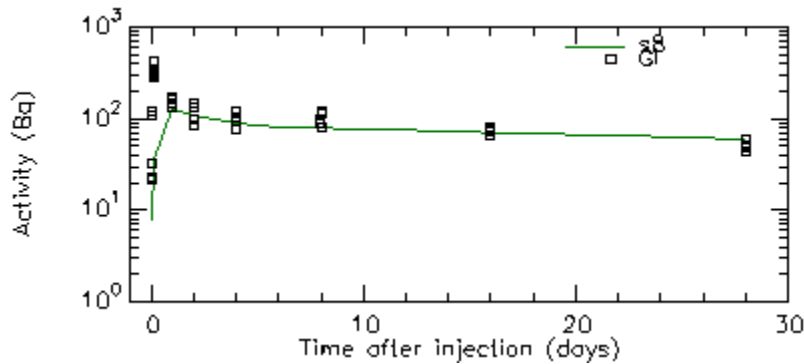


**Figure 18.** Semilog plot of GI sample in first constructed model.

A plot of the feces sample can be seen in Figure 19. The fit of this curve aligns relatively closely with data points across the entire time period. The one exception is the curve does not quite rise fast enough at a few of the early data points but overall represents a good fit.

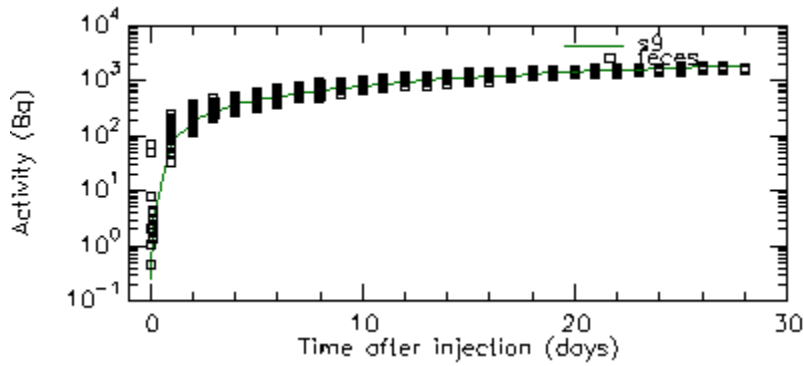


**Figure 19.** Semilog plot of feces sample in first constructed model.

A plot of the pelt sample can be seen in Figure 20. The curve does not fit well to the early data points. It starts out low and does not reach the early activity levels. It instead begins a slow rise and not until about day 8 does the curve start to fit the data.

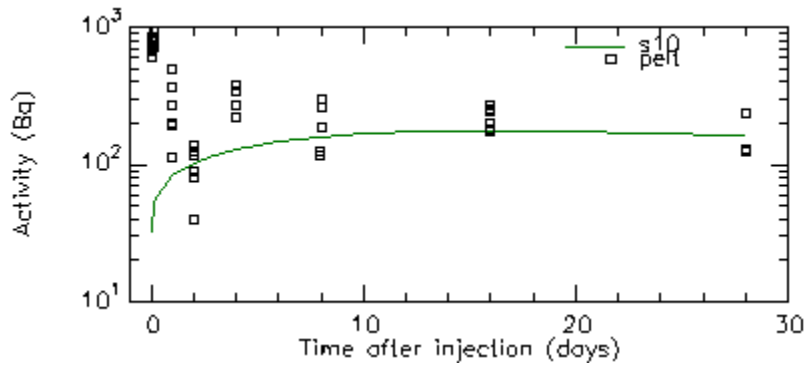


**Figure 20.** Semilog plot of pelt sample in first constructed model.

A plot of the spleen sample can be seen in Figure 21. The curve fits to the data fairly well for the earliest time periods. However, it falls off faster than the data does and continues to underestimate the plot for the remaining time periods.

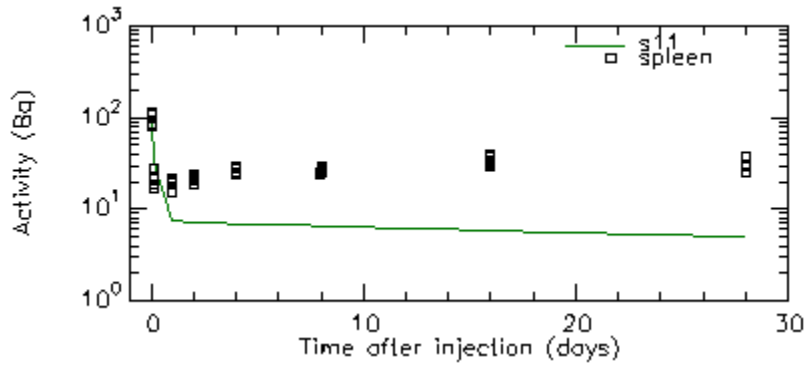


**Figure 21.** Semilog plot of spleen sample in first constructed model.

A plot of the lungs sample can be seen in Figure 22. The fit does not reach the activity levels of the early data points. It does align well with the later time periods and fits with the data fairly well.

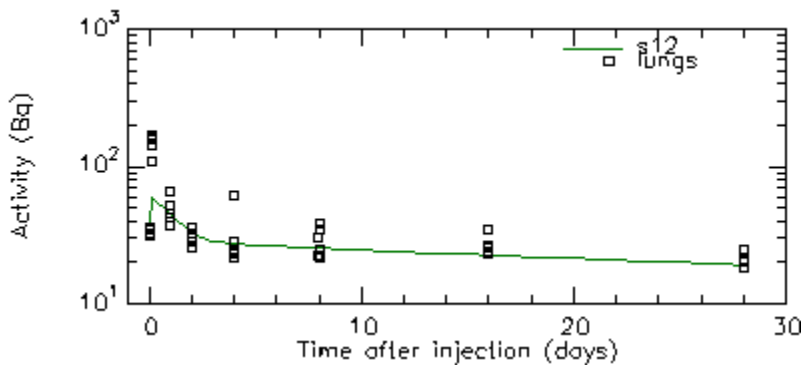


**Figure 22.** Semilog plot of lungs sample in first constructed model.

A plot of the muscle sample can be seen in Figure 23. The curve does not fit the earliest data points at all. However, starting with time period of 0.1667 days, the curve follows the data trend fairly closely until the end of the time period.

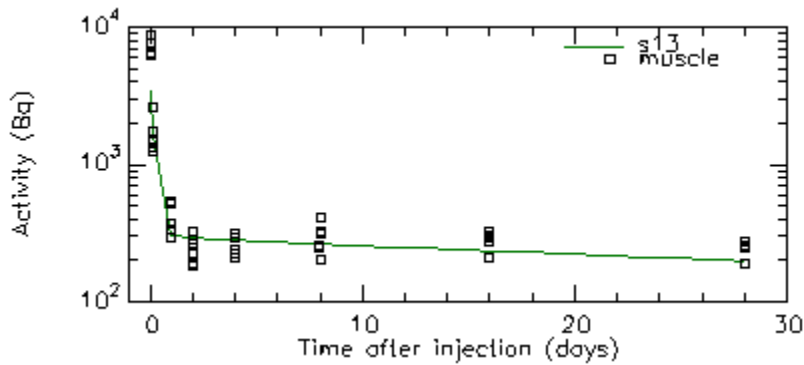


**Figure 23.** Semilog plot of muscle sample in first constructed model.

Overall, each of the sample plots follow the trend of the data reasonably well. There are several samples that either overestimate or underestimate the data, sometimes but a fairly large amount. Multiple plots seem to miss fitting with the earliest time periods, either at 0.04167 days or 0.1667 days. For the key tissue samples being the skeleton and liver, where plutonium is known to accumulate at higher levels than other tissues, the plots are generally poor with representing the data.

#### Reduced Compartmental Model

After the original model, several models were constructed by combining compartments. This final reduced model was constructed in SAAM II by combining the spleen compartment with the liver compartment and the lungs, muscle, pelt, and gonads with the soft tissue compartment. This led to the reduced model as can be seen in Figure 24.

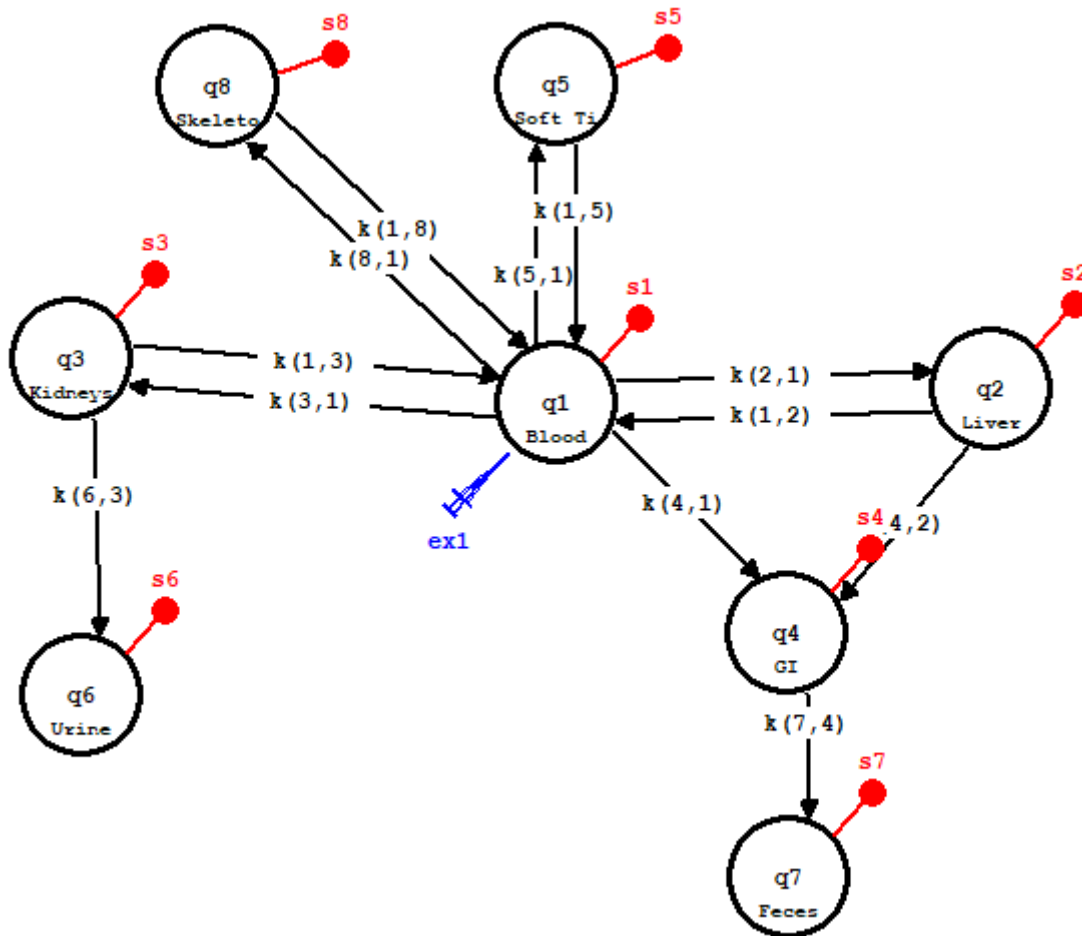


**Figure 24.** Reduced compartment model. The red circles indicate the sample data associated with each compartment. The blue syringe indicates an injection into the blood compartment. The q1, q2, etc. designation in each compartment is how SAAM II represents the compartment.

Each of the compartments show recycling occurring back to the blood compartment apart from the GI, urine, and feces compartments. The parameters were entered into SAAM II for each of the pathways. These parameters were partly based on the previous parameters SAAM II had reported and from the literature of models that had been constructed to determine human transfer rates. The parameters for the reduced compartment model are listed in Table 8.

**Table 8.** Parameters for reduced compartmental model.

Source to Target Organ	Transfer rate (day <sup>-1</sup> )
Liver to Blood	-0.023
Kidneys to Blood	-0.154
Soft tissue to Blood	78.034
Skeleton to Blood	0.013
Blood to Liver	2.465
Blood to Kidneys	0.225
Blood to GI	0.331
Liver to GI	0.071
Blood to Soft tissue	546.829
Kidneys to Urine	0.314
GI to Feces	0.788
Blood to Skeleton	9.818

The AIC/M value calculated by SAAM II is 6.275. The total number of data points  $M$  for this model was 1,010. As defined in the literature, this equates to an AIC value of 12,675.5.

Each of the samples are shown graphically in a semilog plot. The graphs show the amount of activity in Bq versus the time after injection in days. A fit of the data as calculated by SAAM II for each sample based on the parameters of the compartments is also shown. The results for the samples are listed on a tissue by tissue basis.

A plot of the blood sample can be seen in Figure 25. The curve fits the data relatively well though it does drop off quicker than the data points on day 4. This plot does appear to be a better fit than the blood sample plot in the first compartmental model.

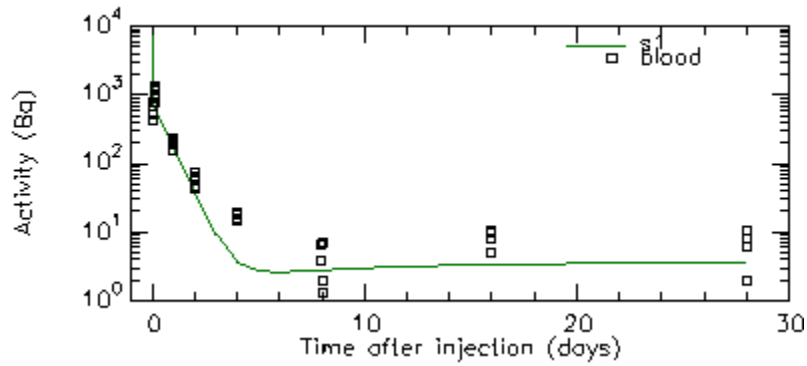


**Figure 25.** Semilog plot of blood sample in reduced compartment model.

A plot of the liver sample can be seen in Figure 26. The curve of this fit aligns relatively closely with the data points with the exception of the data at 0.1667 days. The fit does not quite reach that data before fitting the remaining data. This plot is considerably better than the liver sample plot in the first compartmental model.

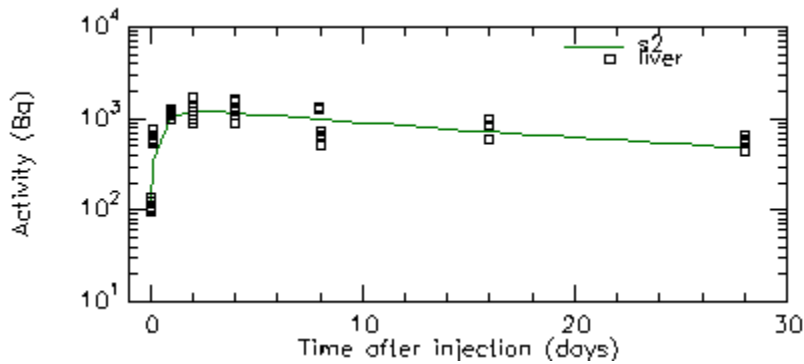


**Figure 26.** Semilog plot of liver sample in reduced compartment model.

A plot of the kidneys sample can be seen in Figure 27. The fit of this plot is relatively poor. The curve misses the initial data points before rising and fitting with the next two sets of data and then dropping off faster than the data suggests. In this case, the kidneys sample in the first compartmental model shows a better fit of the data than this plot does.

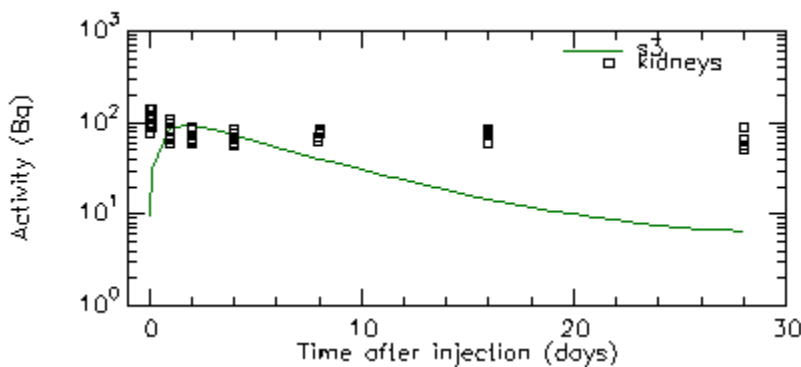


**Figure 27.** Semilog plot of kidneys sample in reduced compartment model.

A plot of the GI sample can be seen in Figure 28. The fit of this plot appears to be very good for the later data points but similar to the GI sample in the first compartmental model, it completely misses fitting to the higher activity levels at 0.1667 days and at 1 day. Starting with the data at day 2, the plot aligns fairly closely with the data.

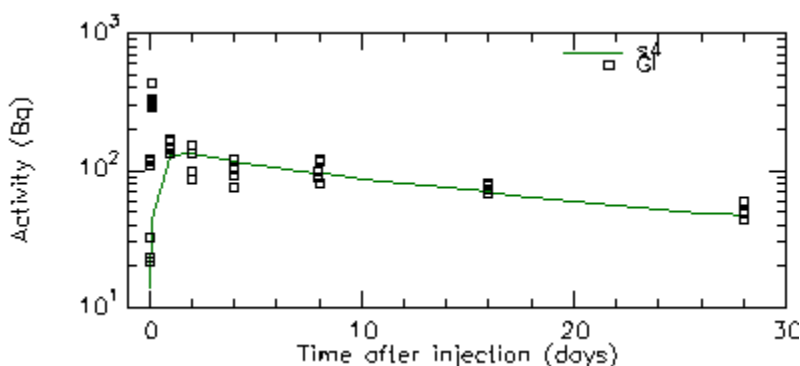


**Figure 28.** Semilog plot of GI sample in reduced compartment model.

A plot of the soft tissue sample can be seen in Figure 29. The fit of the curve appears to be relatively good for the early data points, though it may not be properly fitting the first set of data. However, after day 2, instead of plateauing as the data does, the curve drops and underestimates the data points. The soft tissue sample for the first compartmental model also underestimated the data points, but not to the extreme that this plot does.

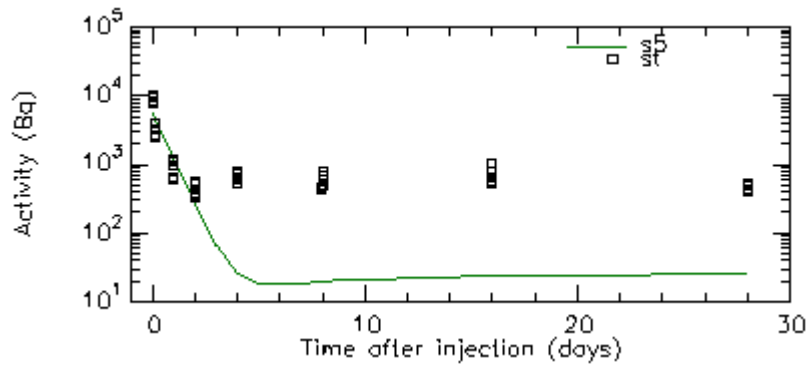


**Figure 29.** Semilog plot of soft tissue sample in reduced compartment model.

A plot of the urine sample can be seen in Figure 30. The fit of the curve appears to align relatively well with the data. The exception to this is the early data. Similar to the urine sample in the first compartment model, the lower activity data point at 0.04167 days may be affecting the fit of the plot.

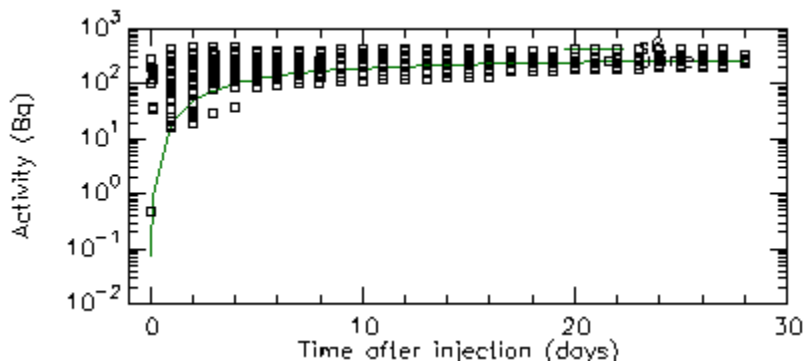


**Figure 30.** Semilog plot of urine sample in reduced compartment model.

A plot of the feces sample can be seen in Figure 31. The fit of this curve follows the data points very well with the one exception of a few of the data at day 1. This plot is very similar to the first compartmental model plot for feces sample.

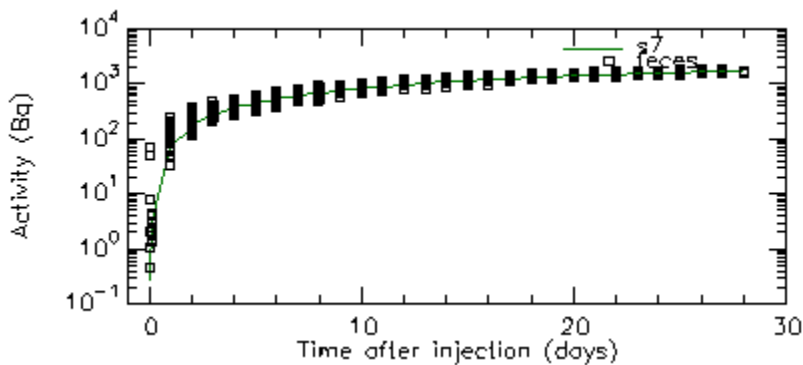


**Figure 31.** Semilog plot of feces sample in reduced compartment model.

A plot of the skeleton sample can be seen in Figure 32. The curve follows the data points relatively though it does not fit to it. After initially underestimating the fit, it overcorrects and overestimates the fit for the remaining time period. It is, however, a better fit than the skeleton compartment in the first compartmental model which overestimated the data from the start and continued the trend for the entire time period in a more exaggerated manner than this plot.

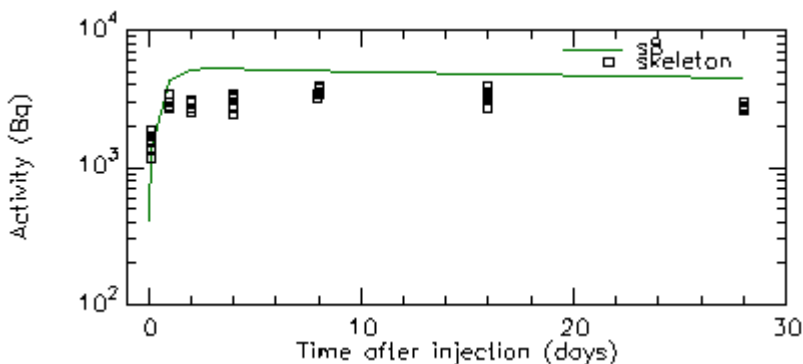


**Figure 32.** Semilog plot of skeleton sample in reduced compartment model.

The sample plots all seem to follow the trend of the data reasonably well. It also appears that the fit of the plots are better in the primary tissues of concern, the skeleton and the liver, though the kidneys and soft tissues samples do not fit as well.

## Two liver compartment model

Complexities were added back into the model by splitting a compartment into multiple compartments. In this case, the liver compartment was separated into two compartments where the recycling back to the blood compartment occurs after traveling through liver 1 and liver 2 and the pathway to the GI comes only from liver 1. The sample data is shared between the liver 1 and liver 2 compartments since the liver samples were not separated into multiple samples. The model can be seen in Figure 33.

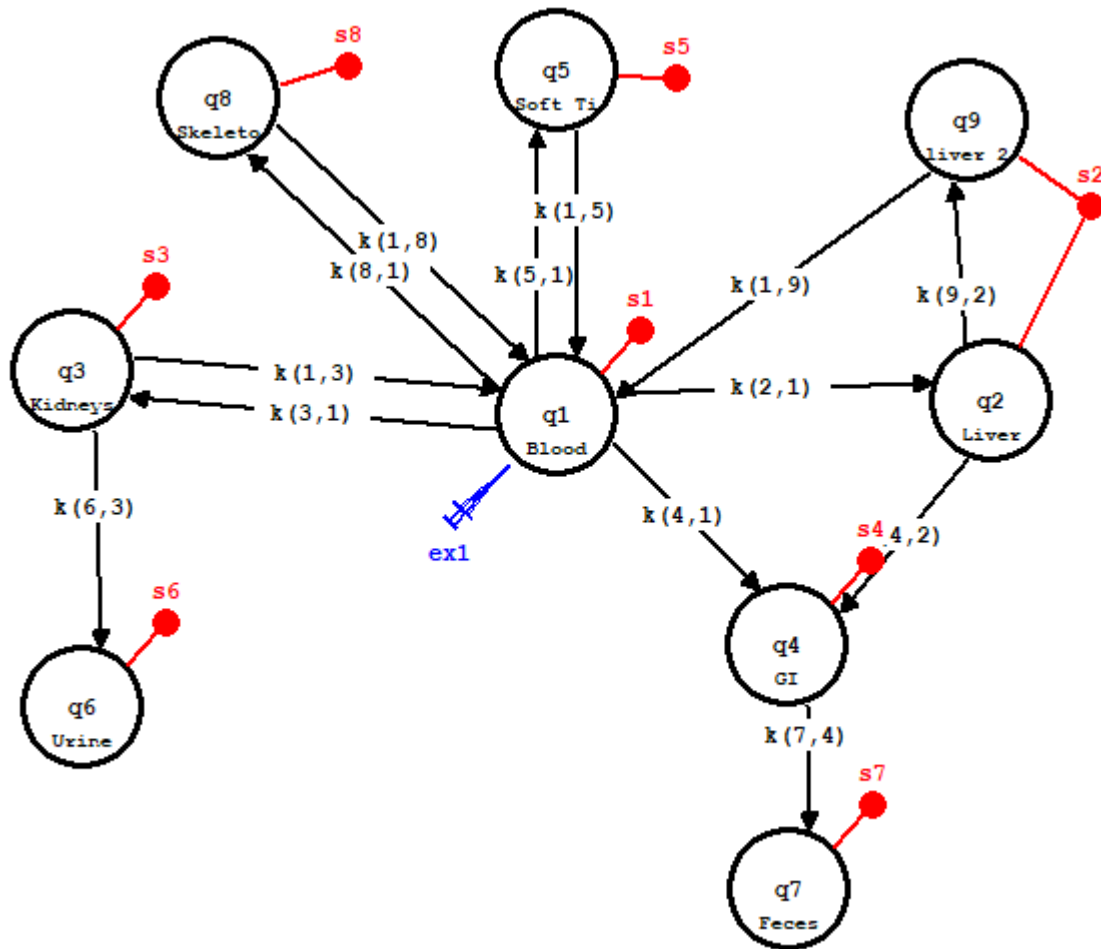


**Figure 33.** Two liver compartment model. The red circles indicate the sample data associated with each compartment. The blue syringe indicates an injection into the blood compartment. The q1, q2, etc. designation in each compartment is how SAAM II represents the compartment.

SAAM II processed the inputted data for the two liver compartment model but had the same issue as the original model in that the covariance matrix was unreliable. This means as the data is not informative enough to allow reliable estimation of the parameters. Typically, the best fix for this issue is to collect more data or simplify the model. The parameters calculated by SAAM II are in Table 9.

**Table 9.** Parameters for two liver compartmental model.

Source to Target Organ	Transfer rate (day <sup>-1</sup> )
Kidneys to Blood	-0.179
Soft tissue to Blood	0.004
Skeleton to Blood	6.89*10 <sup>-4</sup>
Liver 2 to Blood	1.0*10 <sup>5</sup>
Blood to Liver 1	0.017
Blood to Kidneys	0.002
Blood to GI	0.002
Liver 1 to GI	0.082
Blood to Soft tissue	0.008
Kidneys to Urine	0.301
GI to Feces	0.783
Blood to Skeleton	2.639
Liver 1 to Liver 2	-0.044

The AIC/M value calculated by SAAM II is 6.685. The total number of data points  $M$  for this model was 1,010. As defined in the literature, this equates to an AIC value of 13,503.7.

Each of the samples are shown graphically in a semilog plot. The graphs show the amount of activity in Bq versus the time after injection in days. A fit of the data as calculated by SAAM II for each sample based on the parameters of the compartments is also shown. The results for the samples are listed on a tissue by tissue basis.

A plot of the blood sample can be seen in Figure 34. The curve dramatically overestimates the data from the start of the plot. While it does decrease as the data does, it continues to

overestimate the data for the entire period. The fit of this plot is worse than the fit of the blood sample in the reduced compartment model. It is also not a better fit than the blood sample in first compartmental model since that fit underestimated the data as opposed to overestimating the data as this one does.

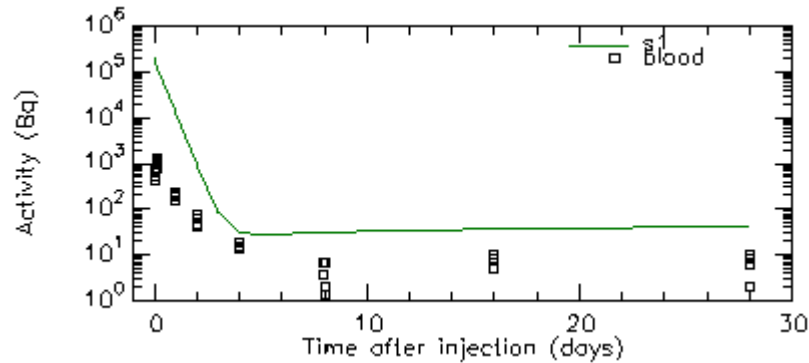


**Figure 34.** Semilog plot of blood sample in two liver compartment model.

A plot of the liver sample can be seen in Figure 35. The fit of this curve aligns very well with the data points. It is similar to the plot of the liver sample in the reduced compartmental model but may fit the early data slightly better.

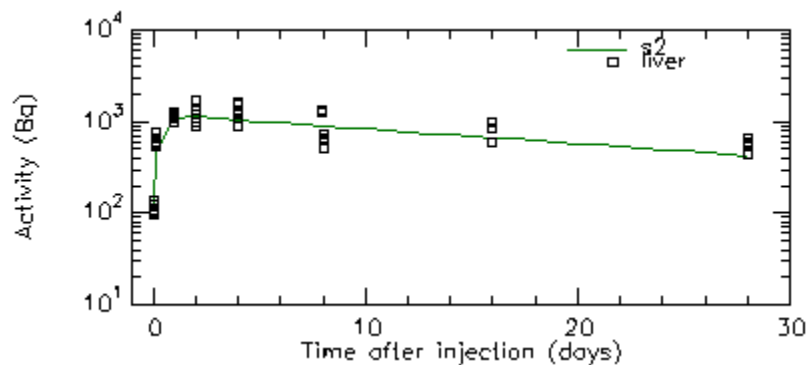


**Figure 35.** Semilog plot of liver sample in two liver compartment model.

A plot of the kidneys sample can be seen in Figure 36. Similar to the kidneys sample in the reduced compartmental model, the fit of the data is poor, though this curve has a more defined

drop off. The kidneys sample for the first compartmental model still has the best fit of the three plots.

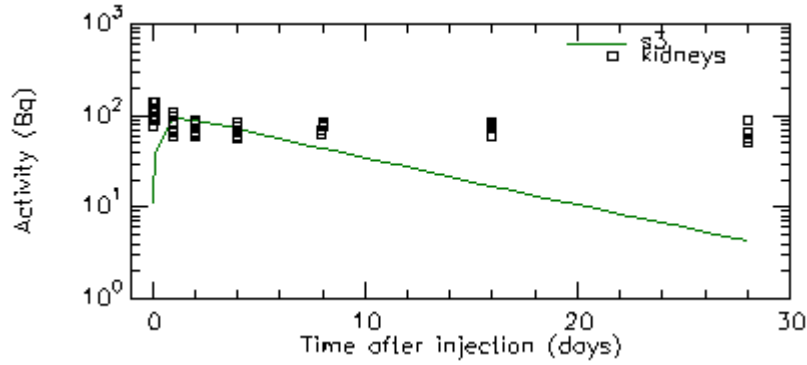


**Figure 36.** Semilog plot of kidneys sample in two liver compartment model.

A plot of the GI sample can be seen in Figure 37. This plot shows a good fit of the later data points but like the previous models, it misses the early data points. The three models all show similar fits of the GI sample data.

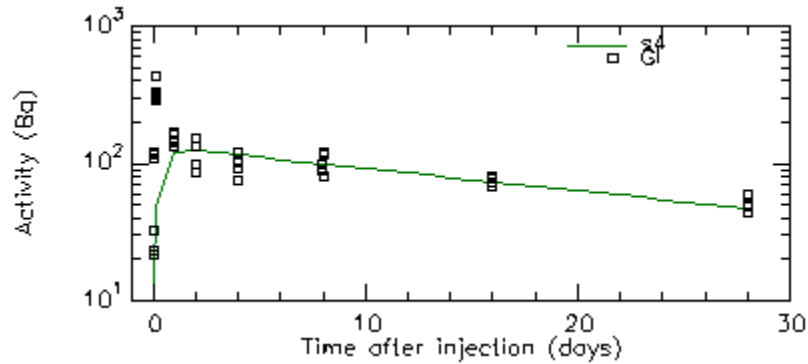


**Figure 37.** Semilog plot of GI sample in two liver compartment model.

A plot of the soft tissue sample can be seen in Figure 38. The fit of the data is very good starting at day 4, but the curve is an inverse of the early data points. The soft tissue sample fits for

the previous two compartment models underestimated the data, but they did follow the trend of the data unlike the fit for this sample.

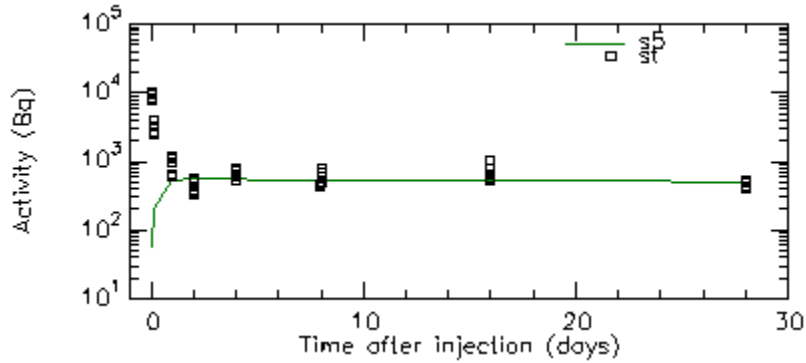


**Figure 38.** Semilog plot of GI sample in two liver compartment model.

A plot of the urine sample can be seen in Figure 39. The fit of this data is good and similar to the urine samples in the previous models. The first low activity data point may be the cause of underestimating the initial data points before fitting well with the later data.

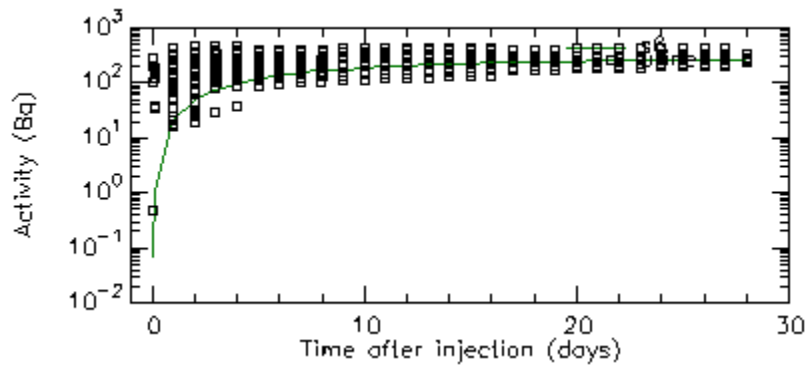


**Figure 39.** Semilog plot of urine sample in two liver compartment model.

A plot of the feces sample can be seen in Figure 40. The fit of this plot is very good and is similar to the feces samples in the previous two models. It is still underrepresenting the data slightly at day 1, but overall is a good fit.

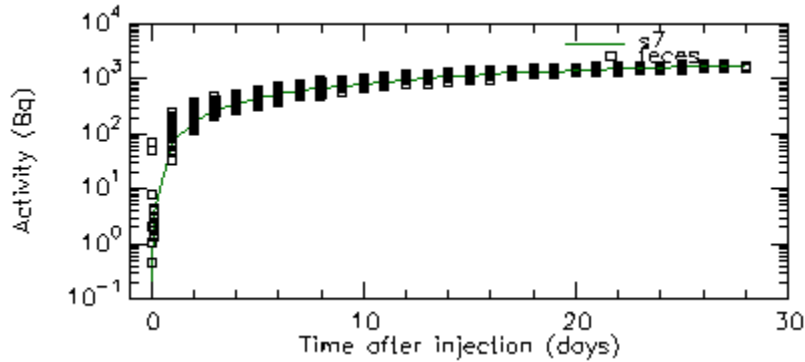


**Figure 40.** Semilog plot of feces sample in two liver compartment model.

A plot of the skeleton sample can be seen in Figure 41. The fit overestimates the data from the beginning and while it does follow the trend of the data, it is considerably larger than the data points represent for the entire time period. The fit for the skeleton sample for the reduced compartment model remains the best fit of the three models.

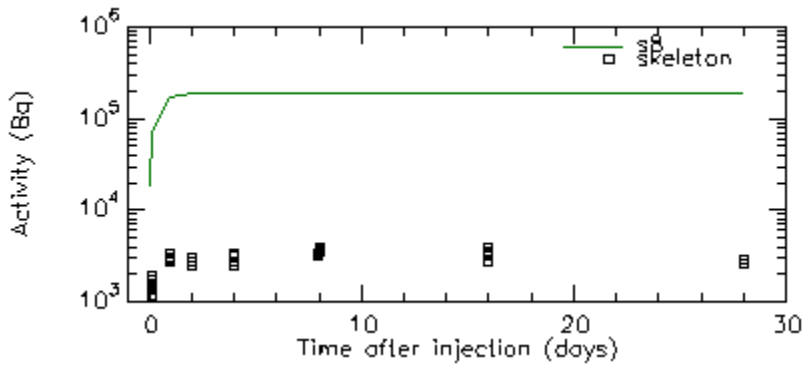


**Figure 41.** Semilog plot of skeleton sample in two liver compartment model.

$\Delta AIC$

The model that had the lowest AIC was the reduced model with a value of 12,675.5 and therefore is the  $AIC_{min}$ . For the first model that was constructed, the AIC was 15,002.5. Calculating the  $\Delta AIC$  from equation 6,

$$\Delta AIC = 15002.5 - 12675.5 \quad (7)$$

$$\Delta AIC = 2327 \quad (8)$$

Since this  $\Delta AIC$  value is greater than 10, there is no support for using this model. The two liver compartment model AIC value was 13,504.4. Using equation 6 again to calculate the  $\Delta AIC$ ,

$$\Delta AIC = 13503.7 - 12675.5 \quad (9)$$

$$\Delta AIC = 828.2 \quad (10)$$

While the  $\Delta AIC$  value for the two liver compartment model is better than the value calculated for the first constructed model, it still has a value greater than 10 and there is no support for using this model.

## CHAPTER 6

### DISCUSSION

The results of this research did not end up as entirely expected. While a more reduced model was hypothesized as being the most likely model to represent a good fit of the data and present a quality of model as represented by AIC, the results only partially reflected this. Several of the compartments did not fit to the data as well as predicted and the AIC values for each of the models were not as low as originally thought they would be. The AIC/M value was lowest for the first compartmental model but due to it having more data points, it had a larger AIC than the reduced compartment model. The reduced compartment model also appears to have better fits of the data overall than the first compartment model, specifically with the liver and skeleton, but it does not apply to all of the compartments.

When reducing the compartments, the spleen was grouped with the liver compartment, while the remaining tissues were grouped with the soft tissue compartment. The spleen appears to act as more of a pass through organ to the liver. The spleen does see a good portion of the blood supply and actinides before passing them through to the liver. Adding the spleen to the liver compartment seems to be a logical choice when reducing the compartments and the fit of the liver data as shown in Figure 26 for the reduced compartment model reflects this as the liver shows a much greater fit in this model than the liver and spleen compartments show in the first constructed model.

It was surprising to see several of the pathways between compartments resulted in negative transfer rates. SAAM II uses linear transfer rates in calculating the parameters for each of the pathways. It is possible that while this method is effective for some pathways, it may not be others. One specific pathway that was unable to find a good fit to the data in any of the models was the kidneys. The fit would change based on how many compartments consisted of the kidneys data and the multiple pathways leading to these compartments, recycling back to the blood, and a pathway to excretion, but it never calculated a good fit to the data. The rate out of the kidneys always showed a faster loss than the data reported. Additional research looking at complex transfer rates may help fit this data, as well as improve the fit of other compartments.

In the literature with regards to humans, there seems to be considerable variability when it comes to retention of activity in the liver and skeleton, with often times the liver showing a higher amount of activity in the early time periods before decaying and a gradual shift to the amount of activity in the skeleton in the later time periods. This did not seem to hold true for the rat. The skeleton showed a higher amount of activity from the start than the liver as well as a much slower decay over time. The liver and skeleton compartments are still considered to be the primary areas of interest in the rat as they are with humans, but the retention between the two may not be the same. This could be due to the data from humans coming as adults when they have reached maturity whereas the rats were still young in comparison. A deeper comparison between the two is worth examination in the future.

It should be noted there is a limitation with the data. While the results were deemed acceptable for the study, there is a wide range in the recovered activity fraction between the groups of rats. This could contribute for the issues in aligning the fits for each compartment between the early and later time periods.

## CHAPTER 7

### CONCLUSIONS

A revised systemic biokinetic rat model was developed for  $^{239}\text{Pu}$ . This research suggested that a simpler systemic model may be beneficial for the use in rats. The reduced compartment model had the lowest AIC value indicating the model had the highest quality. The overall fit of the sample data was better than the other models that were constructed. SAAM II was also able to perform a fit of each data sample based on the reduced compartment model while it was unsuccessful for many others. Further research to explore complex transfer rates for certain pathways may lead to a greater fit of the data and an even lower AIC value for the reduced compartment model. It may also be beneficial to conduct additional animal experiments to collect additional tissue and organ samples such as from the bladder, or, being able to differentiate parts of the liver so two sets of samples are collected as opposed to one sample being used and two compartments being developed.

## REFERENCES

- Aho K, Derryberry D, Peterson T. Model selection for ecologists: the worldviews of AIC and BIC. *Ecology* 95: 631-636; 2014.
- Akaike H. A new look at the statistical model identification. *IEEE Transactions on Automatic Control* AC-19: 716-723; 1974.
- Akaike H. Information theory and an extension of the maximum likelihood principle. In: Kotz S, Johnson NL, eds. *Breakthrough in Statistics*. New York, NY; 1992: 610-624.
- Austin AL, Lord BI. A biokinetic model for alpha-emitting bone surface-seeking radionuclides in the mouse skeleton. *Radiation Protection Dosimetry* 92: 233-238; 2000.
- Austin AL, Ellender M, Haines JW, Harrison JD, Lord BI. Microdistribution and localized dosimetry of the alpha-emitting radionuclides  $^{239}\text{Pu}$ ,  $^{241}\text{Am}$ , and  $^{233}\text{U}$  in mouse femoral shaft. *International Journal of Radiation Biology* 76: 101-111; 2000.
- Ballou JE, Thompson RC, Clarke WJ, Palotay JL. Comparative toxicity of plutonium-238 and plutonium-239 in the rat. *Health Physics* 13: 1087-1092; 1967.
- Burnham KP, Anderson DR. *Model selection and multimodel inference: A practical information-theoretic approach*, 2<sup>nd</sup> ed. Springer, New York, NY; 2002.
- Carritt J, Fryxell R, Kleinschmidt J, Kleinschmidt R, Langham W, San Pietro A, Schaffer R, Schnap B. The distribution and excretion of plutonium administered intravenously to the rat. *Journal of Biological Chemistry* 171: 273-283; 1947.
- Dagle GE, Cannon WC, Stevens DL, McShane JF. Comparative disposition on inhaled  $^{238}\text{Pu}$  and  $^{239}\text{Pu}$  nitrates in beagles. *Health Physics* 44: 275-277; 1983.
- deLeeuw J. Introduction to Akaike (1973) Information theory and an extension of the maximum likelihood principle. In: Kotz S, Johnson NL, eds. *Breakthrough in Statistics*. New York, NY; 1992: 599-609.
- Durbin PW, Horovitz MW, Close ER. Plutonium deposition kinetics in the rat. *Health Physics* 22: 731-741; 1972.
- Durbin PW. Plutonium in mammals: influence of plutonium chemistry, route of administration, and physiological status of the animal on initial distribution and long-term metabolism. *Health Physics* 29: 495-510; 1975.

- International Commission on Radiological Protection. Permissible dose for internal radiation. Oxford: Pergamon Press; ICRP Publication 2, 1959.
- International Commission on Radiological Protection. The metabolism of compounds of plutonium and other actinides. Oxford: Pergamon Press; ICRP Publication 19, 1972.
- International Commission on Radiological Protection. The metabolism of plutonium and related elements. Oxford: Pergamon Press; ICRP Publication 48, 1986.
- International Commission on Radiological Protection. Age-dependent doses to members of the public from intake of radionuclides: Part 1. Oxford: Pergamon Press; ICRP Publication 56, 1989.
- International Commission on Radiological Protection. Age dependent dose to members of the public from intake of radionuclides: Part 2 ingestion dose coefficients. Oxford: Pergamon Press; ICRP Publication 67, 1993.
- International Commission on Radiological Protection. Doses to the embryo and fetus from intakes of radionuclides by the mother. Oxford: Pergamon Press; ICRP Publication 88, 2001.
- International Commission on Radiological Protection. Nuclear decay data for dosimetric calculations. Oxford: Pergamon Press; ICRP Publication 107, 2008.
- Langham WH, Bassett SH, Harris PS, Carter RE. Distribution and excretion of plutonium administered intravenously to man. Los Alamos, NM: Los Alamos Scientific Laboratory; LASL Report LA 1151; 20 September 1950. Reprinted in Health Physics 38: 1031-1060; 1980.
- Leggett RW. A model of the retention, translocation and excretion of systemic Pu. Health Physics 49: 1115-1137; 1985.
- Leggett RW, Eckerman KF. Evolution of the ICRP's biokinetic models. Radiation Protection Dosimetry 53: 147-155; 1994.
- Leggett RW, Eckerman KF, Khokhryakov VF, Suslova KG, Krahenbuhl MP, Miller SC. Mayak worker study: an improved biokinetic model for reconstructing doses from internally deposited plutonium. Radiation Research 164: 111-122; 2005.
- Lloyd RD, Miller SC, Taylor GN, Bruenger FW, Angus W, Jee WSS. Comparison of internal emitter radiobiology in animals and humans. Health Physics 72: 100-110; 1997.
- Lloyd RD, McFarland SS, Atherton DR, Mays CW. Plutonium retention, excretion, and distribution in juvenile beagles soon after injection. Radiation Research 75: 633-641; 1978.
- Luciani A, Polig E. Verification and modification of the ICRP-67 model for plutonium dose calculation. Health Physics 78: 303-310; 2000.

- Morin M, Nenot JC, Lafuma J. Metabolic and therapeutic study following administration to rats of  $^{238}\text{Pu}$  nitrate – a comparison with  $^{239}\text{Pu}$ . *Health Physics* 23: 475-480; 1972.
- National Council on Radiation Protection and Measurements. Research needs for radiation protection. Bethesda, MD: NCRP; NCRP Report No. 117, 1993.
- National Council on Radiation Protection and Measurements. Radionuclide exposure of the embryo/fetus. Bethesda, MD: NCRP; NCRP Report No. 128, 1998.
- National Council on Radiation Protection and Measurements. Liver cancer risk from internally-deposited radionuclides. Bethesda, MD: NCRP; NCRP Report No. 135, 2001.
- National Council on Radiation Protection and Measurements. Development of a biokinetic model for radionuclide contaminated wounds and procedures for their assessment, dosimetry and treatment. Bethesda, MD: NCRP; Report No. 156; 2006.
- Pan W. Akaike's information criterion in generalized estimating equations. *Biometrics* 57: 120-125; 2001.
- Polig E. Kinetic model of the distribution of  $^{239}\text{Pu}$  in the beagle skeleton. *Health Physics* 57: 449-460; 1989.
- Polig E. Labels of surface-seeking radionuclides in the human skeleton. *Health Physics* 72: 19-33; 1997.
- Poudel D, Krage ES, Brey RR, Guilmette RA. Comparison of ICRP 67 and other plutonium systemic model predictions with the biokinetic data from nonhuman primates. *Health Physics* 110:361-369; 2016.
- Rosenthal MW, Lindenbaum A, Russell JJ, Moretti E, Chladek D. Metabolism on monomeric and polymeric plutonium in the rabbit; comparison with the mouse. *Health Physics* 23: 231-238; 1972.
- Schubert J, Finkel MP, White MR, Hirsch GM. Plutonium and yttrium content of the blood, liver, and skeleton of the rat at different times after intravenous administration. *Journal of Biological Chemistry* 182: 635-642; 1950.
- Scott KG, Axelrod DJ, Fisher H, Crowley JF, Hamilton JG. The metabolism of the plutonium in rats following intramuscular injection. *Journal of Biological Chemistry* 176: 283-293; 1948.
- Seaborg GT, McMillan EM, Kennedy JW, Wahl AC. Radioactive element 94 from deuterons on uranium. *Physical Review* 69: 366-367; 1946.

- Shleien B, Slaback Jr LA, Birky BK. Handbook of health physics and radiological health. Third edition. Baltimore, MD: Williams and Wilkens; 1998.
- Stanley JA, Edison AF, Mewhinney JA. Distribution, retention and dosimetry of plutonium and americium in the rat, dog and monkey after inhalation of an industrial-mixed uranium and plutonium oxide aerosol. Health Physics 43: 521-530; 1982.
- Stather JW, Howden S. The effect of chemical form on the clearance of <sup>239</sup>-plutonium from the respiratory system of the rat. Health Physics 28: 29-39; 1975.
- Talbot RJ, Knight DA, Morgan A. Biokinetics of <sup>237</sup>Pu citrate and nitrate in the rat: implications for Pu studies in man. Health Physics 59: 183-187; 1990.
- Taylor DM. Chemical and physical properties of plutonium. In Uranium, Plutonium, Transuranic elements. Eds: Hodge HC, Stannard JN, Hirsch JB. Springer – Verlag, Heidelberg: 323-347; 1973.
- Taylor DM. Some aspects of the comparative metabolism of plutonium and americium in rats. Health Physics 8: 673-677; 1962.
- Taylor DM. The comparative retention of bone-seeking radionuclides in the skeletons of rats. Health Physics 45: 768-772; 1983.
- Taylor DM. The uptake, retention and distribution of plutonium-239 in rat gonads. Health Physics 32: 29-31; 1977.
- The Epsilon Group. SAAM II [online]. 2017. Available at <https://tegvirginia.com/software/saam-ii>. Accessed 4 June 2020.
- Turner GA, Taylor DM. The transport of plutonium, americium, and curium in the blood of rats. Physics in Medicine and Biology 13: 535-546; 1968.
- Weber WM. Model validation study of intravenously injected plutonium-239 in rats. Personal Communication: 2 April 2019.

## APPENDIX A

There was a total of 16 unique models developed but only three of these were discussed as part of the results. Since most of the models were not able to produce any results, they were not previously discussed. Three additional models are shown here as well as brief explanation of what each represents and the reason they were ultimately not discussed in the body of the paper.

The first model is similar to the two liver compartment model except this show two compartments for the kidneys and can be seen in Figure A.1. None of the models developed had shown a good fit of the data for the kidneys so a second compartment was added in the hopes it produces an improved fit. This second compartment while not specifically defined, was thought to represent the renal tubules.

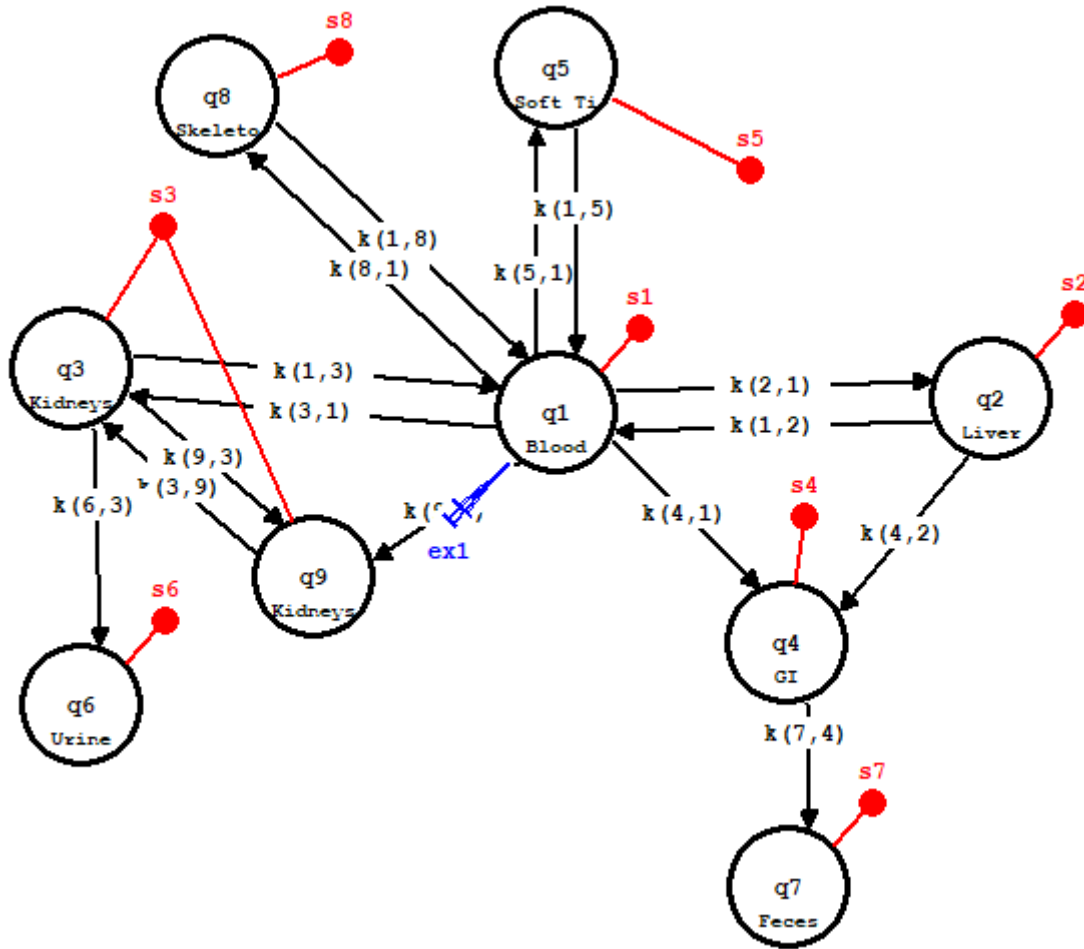


**Figure A.1.** Two kidneys compartment model.

Multiple pathway options between the blood, the two kidneys compartments, and the blood were used in to determine if this model would provide a good fit for the kidneys data. Parameters were used in to determine if this model would provide a good fit for the kidneys data. Parameters were also changed repeatedly. Each iteration was unable to find any combination of parameter values that would enable the model to converge. After trying different scenarios for this model, it was decided that this model would not work in the development of systemic rat model.

The next model developed was a two soft tissue compartment model. Again, similar to the two liver and two kidneys compartment models, this model broke the soft tissue compartment into two compartments and an example of this can be seen in Figure A.2. In the literature, multiple

compartment models are used for humans. The fit for the soft tissue compartments did not provide great fits in previous models so both two compartments and three compartments for the soft tissue was constructed to examine whether the literature models may apply to the rat as well. Only the two compartment soft tissue model is shown.

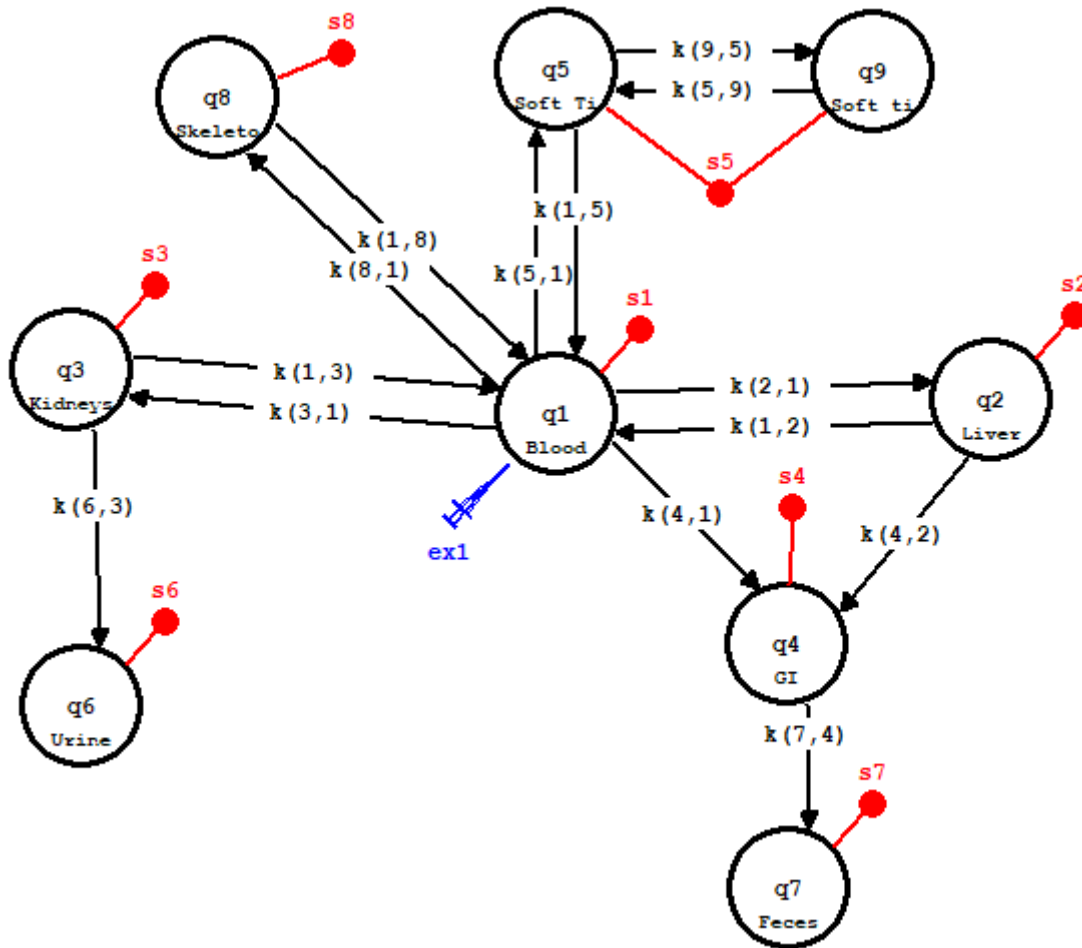


**Figure A.2.** Two soft tissue compartment model.

In the case of both the two soft tissue and three soft tissue compartment models, SAAM II processed the data and reached the 50 iterations which is the maximum number allowed by the software before it stops trying to converge the data. The pathways between the soft tissue compartments and blood were changed as were the parameters values. In each case, the models

were considered unreliable. After multiple attempts to change pathways and parameters without success, it was decided this specific model would not apply to the systemic rat model.

The last model discussed involves adding multiple complexities to the model after the reduced model was produced. Two liver compartments, two kidneys compartments, and two blood compartments were constructed. While not identical, the basis for this model came from Leggett et al. revision of the ICRP 67 model (2005) and can be seen in Figure A.3. Apart from the two liver compartment model, none of the other tissues that were divided into multiple compartments had produced a viable result. Instead of trying to only add one complexity at a time when adding a second compartment for an organ, multiple complexities were added at once to determine if the model needed more compartments to provide better fits for the data.

